Ecole et Observatoire
des Sciences de la Terre

UNIVERSITÉ DE STRASBOURG

Modes normaux de modèles de Terre en rotation

Normal modes of rotating Earth models

Mémoire présenté en vue de l'obtention du diplôme
d'Habilitation à Diriger des Recherches

Discipline : Géophysique

par

Yves Rogister

soutenu le premier octobre 2012 à l'Ecole et Observatoire des Sciences de la Terre
devant le jury composé de

Michel Cara	Professeur, Université de Strasbourg	Rapporteur
Jacques Hinderer	Directeur de Recherches, CNRS-Université de Strasbourg	Examinateur
Michel Rieutord	Professeur, Observatoire Midi-Pyrénées	Rapporteur
Harald Schuh	Professeur, Technische Universität Wien	Rapporteur
Rudolf Widmer-Schnidrig	Professeur, Universität Stuttgart	Examinateur

Table des matières

Les titres de section en *italique* sont ceux d'articles qui ont été publiés.

[...] pour les adeptes de la culture rationnelle que nous sommes depuis la Renaissance, le monde reste une énigme. Il est neuf chaque jour, et il nous appartient de le déchiffrer. C'est notre affaire, à nous les vivants, d'interroger ce mystère. Et même si nous échouons finalement, au moins aurons-nous livré bataille. Nous nous serons efforcés de percer l'énigme à quoi le monde et nos vies s'apparentent. On aura l'éternité pour se reposer de nos peines.

Pierre Bergounioux

Faulkner disait que nous disposons tous d'un territoire pas plus grand qu'un timbre-poste, et que ce qui importe n'est pas la superficie, mais la profondeur à laquelle on creuse. Mon timbre-poste est minuscule. Je ne sais pas si je le creuse bien.

Le roi vient quand il veut, Pierre Michon

Chapitre 1

Introduction

1.1 Modes normaux

Les modes normaux d'un système mécanique, ou oscillations libres, ou vibrations propres, sont les oscillations temporellement sinusoïdales que ce système effectue lorsqu'il ne subit pas l'action continue d'une force extérieure mais qu'il a été excité instantanément. Un mode normal est caractérisé par une fréquence d'oscillation, dite fréquence propre, un temps d'amortissement et un champ des déplacements des particules matérielles constituant le système. Ces caractéristiques ne dépendent que de la forme, de la taille et des propriétés physiques du corps telles que, par exemple, la densité, l'élasticité ou le magnétisme. L'amplitude de l'oscillation, elle, dépend de la source excitatrice. Quand celle-ci n'est pas instantanée mais qu'elle est sinusoïdale et que sa fréquence est égale à une fréquence propre, le corps entre en résonance.

La Terre, qui est un milieu continu déformable et limité dans l'espace, possède une infinité de modes propres. Leur mesure et leur connaissance fournissent donc des informations essentielles sur la forme, la structure et les propriétés physiques de la planète.

Dans l'approximation d'un modèle de Terre sphérique en équilibre hydrostatique composé d'une graine solide entourée d'un noyau liquide lui-même inclus dans le manteau solide, le spectre de ses modes propres comprend les modes sismiques et le spectre du noyau liquide.

Des centaines de modes sismiques ont été observés depuis les années 1960. Sauf pour un mode particulier appelé mode de Slichter dont le déplacement propre est une translation de la graine dans le noyau liquide, les périodes des modes sismiques sont inférieures à une heure environ. Leur qualification de *sismiques* est liée à la nature de leur source excitatrice, les séismes. Depuis 1998, les observations sismologiques montrent toutefois que des modes sismiques sont continûment excités, sans doute par l'atmosphère et les océans.

Le spectre associé au noyau liquide d'un modèle de Terre sphérique est constitué de modes dont les déplacements propres sont confinés dans le noyau liquide et dont les périodes propres sont déterminées par la stratification thermique du noyau, c'est-à-dire l'écart entre le gradient de température réel et le gradient de température adiabatique. La stratification thermique peut aussi s'exprimer en fonction de la densité, du gradient de la densité, de la gravité et de la vitesse des ondes de compression. Comme les déplacements propres des modes du noyau sont quasi-nuls dans le manteau, la détection de ces modes au moyen de sismomètres est peu probable. Néanmoins, on

peut espérer mesurer, à la surface terrestre, les variations de gravité associées aux modes du noyau, pour autant bien entendu qu'ils soient suffisamment excités.

Lorsque la rotation de la Terre sur elle-même n'est plus négligée, sa forme d'équilibre n'est plus sphérique mais elle est légèrement aplatie aux pôles, l'aplatissement étant environ 1/300. La rotation et l'aplatissement ont trois effets sur le spectre des mouvements libres.

Premièrement, la dégénérescence des fréquences propres sismiques est levée, de manière analogue à l'effet Zeeman en mécanique quantique qui lève la dégénérescence des niveaux d'énergie de l'atome d'hydrogène. L'écart relatif entre une fréquence dégénérée et les fréquences éclatées qui en émanent est petit, de l'ordre de l'aplatissement au plus.

Deuxièmement, le spectre du noyau liquide est altéré et contient une composante continue.

Troisièmement, il naît une catégorie de modes supplémentaires, dits modes de rotation. Leurs déplacements propres sont principalement des rotations quasi-rigides des trois couches formant l'intérieur de la Terre autour d'axes équatoriaux. Une première approche, simplifiée, permet de dénombrer quatre modes de rotation : le mouvement de Chandler, la nutation libre du noyau liquide, la nutation libre de la graine et le mouvement de Chandler de la graine. Seuls les deux premiers modes sont indubitablement observés, le mouvement de Chandler l'étant même depuis plus de 120 ans dans les données du mouvement du pôle. L'annonce il y a une dizaine d'années de l'observation de la nutation libre de la graine grâce à l'interférométrie à très longue base (VLBI) n'a pas été unanimement acceptée. Le mouvement de Chandler de la graine n'a, quant à lui, jamais été observé. Il est remarquable que, controversées ou non, les périodes observées sont significativement différentes des périodes prédites pour des modèles de Terre élastiques en équilibre hydrostatique.

1.2 Plan du travail

Ce travail se compose de trois types d'études : des études théoriques où sont établies les équations des déformations de modèles de Terre en rotation, des études numériques où sont calculés des modes normaux, et des études comparatives où des points particuliers des deux types d'études précédents sont expliqués par analogie ou par comparaison avec d'autres théories ou d'autres phénomènes physiques présentant des caractéristiques semblables.

Les études théoriques sont consacrées aux équations locales des petites déformations gravito-élastiques de modèles terrestres en équilibre hydrostatique en rotation (Chapitre 2). Ceux-ci sont calculés à partir de modèles moyens sphériques obtenus par inversion de données géodésiques et sismologiques. En se basant sur la théorie des figures d'équilibre hydrostatique, deux approches sont envisagées pour décrire la perturbation conduisant des modèles sphériques aux modèles aplatis en rotation : l'approche eulérienne et l'approche lagrangienne. La première, développée par ailleurs, a fait l'objet de légères corrections dont certaines sont détaillées dans la Section 2.2. La seconde, l'approche lagrangienne, est entièrement contruite dans la Section 2.3. Pour les deux approches, le champ des déplacements et la variation de gravité sont projetés sur la base des harmoniques sphériques (ou, éventuellement, des harmoniques sphériques généralisées) pour transformer les équations aux dérivées partielles en équations différentielles ordinaires. À la fin de cette première partie, la Section 2.4 décrit comment inclure l'effet du champ magnétique terrestre dans les équations de mouvement.

Les résultats des calculs numériques sont exposés au Chapitre 3. L'éclatement des fréquences

des modes sismiques, dégénérées pour les modèles de Terre sphériques, est étudié dans la Section 3.1.4. Les modes de Slichter sont inclus dans le spectre des modes sismiques. Les résultats concernant les modes de rotation, en particulier le phénomène de croisement évité (*avoided crossing*) générant des mouvements de Chandler doubles ou des mouvements de Chandler de la graine multiples, sont rapportés dans les Sections 3.2.2, 3.2.3 et 3.2.4.

Enfin, les comparaisons avec des modélisations et des systèmes physiques différents sont faites dans la Section 3.1.2 et dans les Chapitres 4 et 5. Plus précisément, dans la Section 3.1.2 on montre comment la fréquence d'oscillation d'une masse attachée à l'extrémité d'un ressort linéaire est éclatée en trois fréquences propres distinctes lorsque le mouvement de la masse est observé dans un système de référence en rotation. Dans le Chapitre 4, on compare les modélisations locales du mouvement présentées dans le Chapitre 2 avec la classique approche globale fondée sur la conservation du moment cinétique de la Terre. Dans le Chapitre 5, on décrit quatre exemples de croisements évités concernant des systèmes vibratoires différents : deux circuits électriques LC couplés, un ion diatomique, des ondes de gravité à la surface d'un océan et la dynamo terrestre. Une alternative au croisement évité des fréquences propres est fournie par leur jonction qui fait apparaître une fréquence propre complexe pouvant caractériser une instabilité.

La liste des références citées en dehors des articles se trouve aux pages 53-55. Les sections dont les titres sont écrits en *italique* contiennent des articles qui ont été publiés dans des revues internationales.

Chapitre 2

Théorie des déformations gravito-élastiques d'un modèle de Terre en rotation

2.1 Introduction

Les modèles de Terre fournis par la sismologie et la géodésie sont des modèles moyens à symétrie sphérique. Un modèle de Terre en rotation est obtenu en perturbant un modèle sphérique qui est supposé être un fluide incompressible. Les modèles initial et final sont en équilibre hydrostatique. En première approximation, une planète en rotation en équilibre hydrostatique prend la forme d'un ellipsoïde aplati aux pôles. Bien que plusieurs types de perturbations peuvent être considérées, la perturbation lagrangienne, en suivant une particule matérielle qui se déplace, et la perturbation eulérienne, en fixant un point géométrique de l'espace, sont les plus courantes.

La théorie des petites déformations de modèles de Terre en rotation développée par Smith (1974) est basée sur une perturbation eulérienne d'un modèle de Terre sphérique à laquelle se superpose la déformation du modèle en rotation obtenu par perturbation du modèle sphérique. Cette déformation du modèle en rotation peut être un mode normal ou toute déformation forcée. Indépendamment de Schastok (1997), j'ai montré que pour étudier les modes de rotation il est insuffisant de supposer que la perturbation transformant un modèle sphérique en un modèle en rotation est du premier ordre en l'aplatissement (Rogister 2001, Section 2.2). Elle doit en effet inclure des termes du *second ordre* en l'aplatissement, en particulier dans les développements de la densité et du potentiel gravifique en polynômes de Legendre.

Avec Michael Rochester, de la Memorial University of Newfoundland and Labrador au Canada, nous avons construit une théorie des petites déformations de modèles de Terre en rotation fondée sur une perturbation *lagrangienne* d'un modèle sphérique pour obtenir un modèle aplati en rotation, lequel subit ensuite une petite déformation, libre ou forcée (Rogister et Rochester 2004, Section 2.3). Cela implique d'écrire les équations de mouvement dans un système de coordonnées non-orthogonales q, χ, ν tel que les paramètres du modèle terrestre de référence sont constants sur les surfaces $q =$ constante. Ces coordonnées sont reliées aux coordonnées sphériques habituelles r, θ, φ par $r = q + h$, $\theta = \chi$ et $\varphi = \nu$, où h est l'écart entre le modèle sphérique de référence et le modèle

en rotation correspondant. Bien sûr, dans ce cas-ci aussi, il est nécessaire de pousser le calcul de la perturbation jusqu'au second ordre en l'aplatissement, c'est-à-dire le second ordre en h. Il y a deux principaux avantages à considérer une perturbation lagrangienne du modèle sphérique de référence plutôt qu'une perturbation eulérienne. Le premier est que les dérivées des paramètres physiques, par exemple la densité et les paramètres de Lamé, qui sont mal contraintes par les observations, n'apparaissent pas dans les équations de mouvement. Le second avantage est que les conditions de continuité et les conditions aux limites du problème des déformations s'écrivent simplement sur des surfaces sphériques.

Afin d'estimer l'effet du champ magnétique terrestre sur les modes normaux, il est nécessaire d'inclure la force de Lorentz dans les équations de mouvement et d'ajouter aux équations décrites dans les deux précédentes sections les équations de Maxwell. Ce travail constituera la Section 2.4, dans laquelle nous utiliserons les coordonnées sphériques r, θ, φ plutôt que les coordonnées q, χ, ν.

2.2 *On the diurnal and nearly diurnal free modes of the Earth*

This paper has been published in 2001 in Geophysical Journal International (**144**, 459–470).

2.3 *Normal-mode theory of a rotating earth model using a Lagrangian perturbation of a spherical model of reference*

This paper, written in collaboration with Michael Rochester, has been published in 2004 in Geophysical Journal International (**159**, 874–908).

2.4 Adding the Lorentz force

The object of this section is to include the Lorentz force in the equations of motion and to take into account Maxwell's equations for the Earth's electromagnetic field. We will enumerate the approximations and hypotheses leading to a set of ordinary differential equations for the small velocity field and magnetic perturbation that superpose on the prescribed velocity and magnetic fields a geodynamo model provides. Solving these ODEs would allow us to estimate the effect of the magnetic field on the Earth normal modes. In particular, an attempt could be made to provide an explanation for the observation of the anomalous splitting of normal modes sensitive to the structure of the core.

Similar equations as those given in Sections 2.4.1 - 2.4.5 and appropriate boundary conditions were derived by Huang et al. (2011) to estimate the effect of the magnetic field on the rotational modes and forced nutations. The results validate former studies (Buffett 1992, Buffett et al. 2002) based on the angular momentum approach, which we will describe in Chapter 4.

Besides, Ivers and Phillips (2008) have established the equations of rotating magnetohydrodynamics in vector spherical harmonics. Their calcultation also includes the heat equation and the viscosity in the equation of motion but neglects the gravity variation.

2.4.1 Maxwell's equations

In order to take into account the influence of the magnetic induction $\mathbf{B}$ on the Earth's normal modes, we add the Lorentz force $\mathbf{j} \times \mathbf{B}$ into the equation for conservation of linear momentum, where $\mathbf{j}$ denotes the electrical current density. Moreover, $\mathbf{B}$ and the electric field $\mathbf{E}$ are solutions of Maxwell's equations :

$$\boldsymbol{\nabla} \cdot \mathbf{D} = \rho_e, \tag{2.1}$$

$$\boldsymbol{\nabla} \times \mathbf{E} = -\frac{\partial \mathbf{B}}{\partial t} \tag{2.2}$$

$$\boldsymbol{\nabla} \cdot \mathbf{B} = 0, \tag{2.3}$$

$$\boldsymbol{\nabla} \times \mathbf{H} = \mathbf{j} + \frac{\partial \mathbf{D}}{\partial t} \tag{2.4}$$

where

$$\mathbf{D} = \epsilon \mathbf{E} \qquad \text{(1st constitutive relationship)} \tag{2.5}$$

is the electrical displacement and ϵ is the electrical permittivity, and

$$\mathbf{B} = \mu \mathbf{H} \qquad \text{(2nd constitutive relationship)}, \tag{2.6}$$

where $\mathbf{H}$ is the magnetic field and μ, the magnetic permeability. ρ_e, which is the charge density, and $\mathbf{j}$ are the sources for the fields.

Approximations and hypotheses 1 to 4

To simplify, we will make the following approximations and hypotheses :

1. There is no charge density : $\rho_e = 0$
2. $\mathbf{j}$ is given by Ohm's law :

$$\mathbf{j} = \sigma(\mathbf{E} + \mathbf{V} \times \mathbf{B}) \qquad \text{(3rd constitutive relationship)}. \tag{2.7}$$

3. The characteristic speeds involved in the problem are much less than the speed of light. Therefore, we neglect the term $\partial \mathbf{D}/\partial t$ in (2.4).
4. The magnetic permeability is vacuum's : $\mu = \mu_0$.

2.4.2 Lorentz force

Consequently, $\mathbf{E}$ is given by

$$\mathbf{E} = \frac{1}{\sigma \mu_0} \boldsymbol{\nabla} \times \mathbf{B} - \mathbf{V} \times \mathbf{B} \tag{2.8}$$

and, if σ is constant, we have

$$\frac{\partial \mathbf{B}}{\partial t} = \boldsymbol{\nabla} \times (\mathbf{V} \times \mathbf{B}) - \frac{1}{\sigma \mu_0} \boldsymbol{\nabla} \times (\boldsymbol{\nabla} \times \mathbf{B}). \tag{2.9}$$

We then decompose the magnetic field into the sum of a main stationary field $\mathbf{B}_0$ and a small field $\mathbf{b}$:

$$\mathbf{B} = \mathbf{B}_0 + \mathbf{b}. \tag{2.10}$$

We also decompose the velocity field into the sum of a stationary field $\mathbf{V}_0$ and a small field $\mathbf{v}$:

$$\mathbf{V} = \mathbf{V}_0 + \mathbf{v}. \tag{2.11}$$

Approximations and hypotheses 5 to 8

5. We linearize Eq. (2.9) and obtain

$$\frac{\partial \mathbf{b}}{\partial t} = \boldsymbol{\nabla} \times (\mathbf{V}_0 \times \mathbf{B}_0) + \boldsymbol{\nabla} \times (\mathbf{V}_0 \times \mathbf{b}) + \boldsymbol{\nabla} \times (\mathbf{v} \times \mathbf{B}_0) - \frac{1}{\sigma\mu_0} \boldsymbol{\nabla} \times [\boldsymbol{\nabla} \times (\mathbf{B}_0 + \mathbf{b})]. \tag{2.12}$$

The stationary fields $\mathbf{B}_0$ and $\mathbf{V}_0$ being related by

$$0 = \boldsymbol{\nabla} \times (\mathbf{V}_0 \times \mathbf{B}_0) - \frac{1}{\sigma\mu_0} \boldsymbol{\nabla} \times (\boldsymbol{\nabla} \times \mathbf{B}_0), \tag{2.13}$$

Eq. (2.12) can be written

$$\frac{\partial \mathbf{b}}{\partial t} = \boldsymbol{\nabla} \times (\mathbf{V}_0 \times \mathbf{b}) + \boldsymbol{\nabla} \times (\mathbf{v} \times \mathbf{B}_0) - \frac{1}{\sigma\mu_0} \boldsymbol{\nabla} \times (\boldsymbol{\nabla} \times \mathbf{b}). \tag{2.14}$$

6. Because the conductivity in the core is large, we neglect the third term on the right-hand side of the last equation.
7. Below, we will also assume that $\mathbf{b}$ and $\mathbf{v}$ are oscillatory fields, so that

$$\frac{\partial \mathbf{b}}{\partial t} = i\omega \mathbf{b} = \boldsymbol{\nabla} \times (\mathbf{V}_0 \times \mathbf{b}) + \boldsymbol{\nabla} \times (i\omega \mathbf{s} \times \mathbf{B}_0), \tag{2.15}$$

where $\mathbf{s}$ is the displacement vector. As there is an imaginary factor $i\omega$ in all but the first term on the right-hand side, the eigenfrequency will be complex.
8. In a first approach, we neglect this term and obtain

$$\mathbf{b} = \boldsymbol{\nabla} \times (\mathbf{s} \times \mathbf{B}_0). \tag{2.16}$$

Now, using Eq. (2.4) and the subsequent approximations to get

$$\mathbf{j} = \frac{1}{\mu_0} \boldsymbol{\nabla} \times \mathbf{B}, \tag{2.17}$$

the Lorentz force can be written

$$\mathbf{j} \times \mathbf{B} = \frac{1}{\mu_0} \left[(\boldsymbol{\nabla} \times \mathbf{B}_0) \times \mathbf{B}_0 + (\boldsymbol{\nabla} \times \mathbf{B}_0) \times \mathbf{b} + (\boldsymbol{\nabla} \times \mathbf{b}) \times \mathbf{B}_0 \right]. \tag{2.18}$$

In the reference state of the outer core, only the first term on the right-hand side appears. Eq. (2.13) shows that the prescribed current convection $\mathbf{V}_0$ in the conducting material is the source

of the magnetic field $\mathbf{B}_0$. Actually, $\mathbf{V}_0$ and $\mathbf{B}_0$ are obtained by solving the geodynamo problem. Of course, the reference state of the outer core is not an equilibrium state. $\mathbf{V}_0$ and $\mathbf{B}_0$ are not stationary fields but they change on a much longer time-scale than the time-scale of the rotational modes that we will consider.

To a obtain a partial differential equation for $\mathbf{v}$, we subtract the equation of motion at instant 0 from the equation of motion at instant t. Consequently, the terms stemming from the Lorentz force are

$$\delta\mathbf{f}_L = \frac{1}{\mu_0}\left[(\boldsymbol{\nabla}\times\mathbf{B}_0)\times\mathbf{b} + (\boldsymbol{\nabla}\times\mathbf{b})\times\mathbf{B}_0\right]. \tag{2.19}$$

The perturbation $\mathbf{b}$ to the magnetic field is given by Eq. (2.16). Moreover, we know from Maxwell's equations that $\mathbf{b}$ is divergence free :

$$\boldsymbol{\nabla}\cdot\mathbf{b} = 0. \tag{2.20}$$

2.4.3 Toroidal, spheroidal and poloidal scalars

Therefore, the spheroidal part of $\mathbf{b}$ only depends on one scalar potential b^P and the total field is the sum of a toroidal field and a poloidal field

$$\mathbf{b} = \boldsymbol{\nabla}\times b^W\mathbf{r} + \boldsymbol{\nabla}\times(\boldsymbol{\nabla}\times b^P\mathbf{r}). \tag{2.21}$$

The same holds for $\mathbf{B}_0$. I anticipate that it may be easier to consider the spheroidal scalars b^U and b^V that determine $\mathbf{b}$:

$$\mathbf{b} = b^U\frac{\mathbf{r}}{r} + \frac{\mathbf{r}}{r}(\boldsymbol{\nabla}\times b^V\mathbf{r}) + \boldsymbol{\nabla}\times b^W\mathbf{r}. \tag{2.22}$$

Eq. (2.20) shows that b^U and b^V depend on each other. Actually, in spherical polar coordinates r, θ, φ, we have

$$\frac{\partial b^U}{\partial r} + \frac{2b^U}{r} + \left(\frac{\partial^2 b^V}{\partial\theta^2} + \frac{\cos\theta}{\sin\theta}\frac{\partial b^V}{\partial\theta} + \frac{1}{\sin^2\theta}\frac{\partial^2 b^V}{\partial\varphi^2}\right) = 0, \tag{2.23}$$

as well as

$$-b^U = \frac{\partial^2 b^P}{\partial\theta^2} + \frac{\cos\theta}{\sin\theta}\frac{\partial b^P}{\partial\theta} + \frac{1}{\sin^2\theta}\frac{\partial^2 b^P}{\partial\varphi^2}, \tag{2.24}$$

$$\frac{\partial b^V}{\partial\theta} = \left(\frac{\partial}{\partial r} + \frac{2}{r}\right)\frac{\partial b^P}{\partial\theta} \tag{2.25}$$

and

$$\frac{\partial b^V}{\partial\varphi} = \left(\frac{\partial}{\partial r} + \frac{2}{r}\right)\frac{\partial b^P}{\partial\varphi}. \tag{2.26}$$

2.4.4 Spherical harmonics expansion

We decompose the vectors in the canonical basis define from the unit vectors of the local basis associated with spherical polar coordinates (Smith 1974).

Approximation or hypothesis 9 and 10

9. We assume that $\mathbf{B}_0$ is axisymmetric, so that its harmonic expansion does not contain harmonic orders different from 0.
10. We neglect the effect of the ellipticity on $\mathbf{B}_0$.

Next, we expand the canonical components in generalized spherical harmonics and obtain from (2.16)

$$
\begin{aligned}
{b^U}_\ell^m = \sum_{\ell'=0}^{\infty} \sum_{\ell''=|\ell-\ell'|}^{\ell+\ell'} & \begin{bmatrix} \ell & \ell' & \ell'' \\ 0 & 0 & 0 \\ m & 0 & m \end{bmatrix} \frac{1}{r} \left[\begin{Bmatrix} L_0^{\ell''} V_{\ell''}^m + 2U_{\ell''}^m \\ 0 \end{Bmatrix} {B_0^U}_{\ell'} + \begin{Bmatrix} U_{\ell''}^m \\ 0 \end{Bmatrix} \left(L_0^{\ell'} {B_0^V}_{\ell'} + 2{B_0^U}_{\ell'} \right) \right] \\
& + \begin{bmatrix} \ell & \ell' & \ell'' \\ 0 & + & - \\ m & 0 & m \end{bmatrix} \frac{1}{r} \left[\begin{Bmatrix} U_{\ell''}^m \\ 0 \end{Bmatrix} {B_0^V}_{\ell'} + \begin{Bmatrix} 0 \\ U_{\ell''}^m \end{Bmatrix} {B_0^W}_{\ell'} + \begin{Bmatrix} V_{\ell''}^m \\ W_{\ell''}^m \end{Bmatrix} {B_0^U}_{\ell'} \right], \qquad (2.27)
\end{aligned}
$$

where

$$
L_i^\ell = \sqrt{\frac{(\ell+i)(\ell-i+1)}{2}}, \qquad (2.28)
$$

$$
\begin{aligned}
{b^V}_\ell^m = \sum_{\ell'=0}^{\infty} \sum_{\ell''=|\ell-\ell'|}^{\ell+\ell'} & \begin{bmatrix} \ell & \ell' & \ell'' \\ + & + & 0 \\ m & 0 & m \end{bmatrix} \left[\begin{Bmatrix} \frac{dU_{\ell''}^m}{dr} + \frac{1}{r}\left(U_{\ell''}^m + L_0^{\ell''} V_{\ell''}^m \right) \\ -\frac{L_0^{\ell''}}{r} W_{\ell''}^m \end{Bmatrix} {B_0^V}_{\ell'} \right. \\
& + \begin{Bmatrix} -\frac{L_0^{\ell''}}{r} W_{\ell''}^m \\ \frac{dU_{\ell''}^m}{dr} + \frac{1}{r}\left(U_{\ell''}^m + L_0^{\ell''} V_{\ell''}^m \right) \end{Bmatrix} {B_0^W}_{\ell'} \\
& \left. + \begin{Bmatrix} U_{\ell''}^m \\ 0 \end{Bmatrix} \frac{d{B_0^V}_{\ell'}}{dr} + \begin{Bmatrix} 0 \\ U_{\ell''}^m \end{Bmatrix} \frac{d{B_0^W}_{\ell'}}{dr} \right] \\
& - \begin{bmatrix} \ell & \ell' & \ell'' \\ + & 0 & + \\ m & 0 & m \end{bmatrix} \left[\begin{Bmatrix} \frac{dV_{\ell''}^m}{dr} + \frac{V_{\ell''}^m}{r} \\ \frac{dW_{\ell''}^m}{dr} + \frac{W_{\ell''}^m}{r} \end{Bmatrix} {B_0^U}_{\ell'} + \begin{Bmatrix} V_{\ell''}^m \\ W_{\ell''}^m \end{Bmatrix} \left(\frac{d{B_0^U}_{\ell'}}{dr} + \frac{L_0^{\ell'}}{r} {B_0^V}_{\ell'} \right) \right. \\
& \left. - \begin{Bmatrix} W_{\ell''}^m \\ V_{\ell''}^m \end{Bmatrix} \frac{L_0^{\ell'}}{r} {B_0^W}_{\ell'} \right] \\
& + \left(\frac{L_2^{\ell''}}{r} \begin{bmatrix} \ell & \ell' & \ell'' \\ + & - & 2 \\ m & 0 & m \end{bmatrix} + \frac{L_2^{\ell'}}{r} \begin{bmatrix} \ell & \ell' & \ell'' \\ + & 2 & - \\ m & 0 & m \end{bmatrix} \right) \left[- \begin{Bmatrix} V_{\ell''}^m \\ W_{\ell''}^m \end{Bmatrix} {B_0^V}_{\ell'} + \begin{Bmatrix} W_{\ell''}^m \\ V_{\ell''}^m \end{Bmatrix} {B_0^W}_{\ell'} \right] \qquad (2.29)
\end{aligned}
$$

and

$$
\begin{aligned}
{b^W}_\ell^m = \sum_{\ell'=0}^{\infty} \sum_{\ell''=|\ell-\ell'|}^{\ell+\ell'} \begin{bmatrix} \ell & \ell' & \ell'' \\ + & + & 0 \\ m & 0 & m \end{bmatrix} \Bigg[& \left\{ \begin{array}{c} \frac{dU^m_{\ell''}}{dr} + \frac{1}{r}\left(U^m_{\ell''} + L_0^{\ell''} V^m_{\ell''}\right) \\ -\frac{L_0^{\ell''}}{r} W^m_{\ell''} \end{array} \right\} {B_0^W}_{\ell'} \\
& + \left\{ \begin{array}{c} -\frac{L_0^{\ell''}}{r} W^m_{\ell''} \\ \frac{dU^m_{\ell''}}{dr} + \frac{1}{r}\left(U^m_{\ell''} + L_0^{\ell''} V^m_{\ell''}\right) \end{array} \right\} {B_0^V}_{\ell'} \\
& + \left\{ \begin{array}{c} U^m_{\ell''} \\ 0 \end{array} \right\} \frac{d{B_0^W}_{\ell'}}{dr} + \left\{ \begin{array}{c} 0 \\ U^m_{\ell''} \end{array} \right\} \frac{d{B_0^V}_{\ell'}}{dr} \Bigg] \\
- \begin{bmatrix} \ell & \ell' & \ell'' \\ + & 0 & + \\ m & 0 & m \end{bmatrix} \Bigg[& \left\{ \begin{array}{c} \frac{dW^m_{\ell''}}{dr} + \frac{W^m_{\ell''}}{r} \\ \frac{dV^m_{\ell''}}{dr} + \frac{V^m_{\ell''}}{r} \end{array} \right\} {B_0^U}_{\ell'} + \left\{ \begin{array}{c} W^m_{\ell''} \\ V^m_{\ell''} \end{array} \right\} \left(\frac{d{B_0^U}_{\ell'}}{dr} - \frac{L_0^{\ell'}}{r} {B_0^V}_{\ell'} \right) \\
& + \left\{ \begin{array}{c} V^m_{\ell''} \\ W^m_{\ell''} \end{array} \right\} \frac{L_0^{\ell'}}{r} {B_0^W}_{\ell'} \Bigg] \\
+ \left(\frac{L_2^{\ell''}}{r} \begin{bmatrix} \ell & \ell' & \ell'' \\ + & - & 2 \\ m & 0 & m \end{bmatrix} + \frac{L_2^{\ell'}}{r} \begin{bmatrix} \ell & \ell' & \ell'' \\ + & 2 & - \\ m & 0 & m \end{bmatrix} \right) & \left[- \left\{ \begin{array}{c} V^m_{\ell''} \\ W^m_{\ell''} \end{array} \right\} {B_0^W}_{\ell'} + \left\{ \begin{array}{c} W^m_{\ell''} \\ V^m_{\ell''} \end{array} \right\} {B_0^V}_{\ell'} \right]
\end{aligned} \tag{2.30}
$$

Arrays with two lines in braces like $\left\{ \begin{array}{c} V^m_{\ell''} \\ W^m_{\ell''} \end{array} \right\}$ mean that the upper line must be choosen if

ℓ' is odd and $|\ell - \ell''|$ is even or zero
or ℓ' is even and $|\ell - \ell''|$ is odd

and the lower line must be choosen if

ℓ' is even and $|\ell - \ell''|$ is even or zero
or ℓ' is odd and $|\ell - \ell''|$ is odd.

Therefore, for a spheroidal (resp. toroidal) magnetic induction of odd (resp. even) degree the coupling chain describing the displacement field is

$$\mathbf{s} = \cdots + \boldsymbol{\sigma}^m_{\ell-2} + \boldsymbol{\tau}^m_{\ell-1} + \boldsymbol{\sigma}^m_{\ell} + \boldsymbol{\tau}^m_{\ell+1} + \boldsymbol{\sigma}^m_{\ell+2} + \cdots \tag{2.31}$$

For a spheroidal (resp. toroidal) magnetic induction of even (resp. odd) degree the coupling chain describing the displacement field is

$$\mathbf{s} = \cdots + \boldsymbol{\tau}^m_{\ell-2} + \boldsymbol{\sigma}^m_{\ell-1} + \boldsymbol{\sigma}^m_{\ell} + \boldsymbol{\sigma}^m_{\ell+1} + \boldsymbol{\tau}^m_{\ell+2} + \cdots \tag{2.32}$$

Symbols like $\begin{bmatrix} \ell & 2 & \ell' \\ 0 & 0 & 0 \\ m & 0 & m \end{bmatrix}$ are numbers called J-squares by Smith (1974). They arise from products of spherical harmonics and involve products of Wigner 3-j symbols.

The perturbation to the Lorentz force is given by

$$-\mu_0\delta f^{U\,m}_{\ell} = \sum_{\ell'=0}^{\infty}\sum_{\ell''=|\ell-\ell'|}^{\ell+\ell'} \begin{bmatrix} \ell & \ell' & \ell'' \\ 0 & + & - \\ m & 0 & m \end{bmatrix} \left[\begin{Bmatrix} b^{V\,m}_{\ell'\,\ell''} \\ b^{W\,m}_{\ell'\,\ell''} \end{Bmatrix} \frac{L_0^{\ell'}}{r} B^{U}_{0\,\ell'} + \begin{Bmatrix} b^{V\,m}_{\ell'\,\ell''} \\ -b^{W\,m}_{\ell'\,\ell''} \end{Bmatrix} \frac{dB^{V}_{0\,\ell'}}{dr} + \begin{Bmatrix} -b^{W\,m}_{\ell'\,\ell''} \\ b^{V\,m}_{\ell'\,\ell''} \end{Bmatrix} \frac{dB^{W}_{0\,\ell'}}{dr} \right.$$
$$+ \begin{Bmatrix} \frac{1}{r}\left(L_0^{\ell''} b^{U\,m}_{\ell'\,\ell''} + 2b^{V\,m}_{\ell'\,\ell''}\right) + \frac{db^{V\,m}_{\ell'\,\ell''}}{dr} \\ -\frac{2}{r} b^{W\,m}_{\ell'\,\ell''} - \frac{db^{W\,m}_{\ell'\,\ell''}}{dr} \end{Bmatrix} B^{V}_{0\,\ell'}$$
$$\left. + \begin{Bmatrix} -\frac{2}{r} b^{W\,m}_{\ell'\,\ell''} - \frac{db^{W\,m}_{\ell'\,\ell''}}{dr} \\ \frac{1}{r}\left(L_0^{\ell''} b^{U\,m}_{\ell'\,\ell''} + 2b^{V\,m}_{\ell'\,\ell''}\right) + \frac{db^{V\,m}_{\ell'\,\ell''}}{dr} \end{Bmatrix} B^{W}_{0\,\ell'} \right], \tag{2.33}$$

$$-\mu_0\delta f^{V\,m}_{\ell} = \sum_{\ell'=0}^{\infty}\sum_{\ell''=|\ell-\ell'|}^{\ell+\ell'} \begin{bmatrix} \ell & \ell' & \ell'' \\ + & 0 & + \\ m & 0 & m \end{bmatrix} \left[\begin{Bmatrix} \frac{1}{r}\left(L_0^{\ell''} b^{U\,m}_{\ell'\,\ell''} + b^{V\,m}_{\ell'\,\ell''}\right) + \frac{db^{V\,m}_{\ell'\,\ell''}}{dr} \\ \frac{b^{W\,m}_{\ell'\,\ell''}}{r} + \frac{db^{W\,m}_{\ell'\,\ell''}}{dr} \end{Bmatrix} B^{U}_{\ell'} + \begin{Bmatrix} b^{W\,m}_{\ell'\,\ell''} \\ b^{V\,m}_{\ell'\,\ell''} \end{Bmatrix} \frac{L_0^{\ell'}}{r} B^{W}_{0\,\ell'} \right]$$
$$+ \begin{bmatrix} \ell & \ell' & \ell'' \\ + & + & 0 \\ m & 0 & m \end{bmatrix} \left[\begin{Bmatrix} b^{U\,m}_{\ell'\,\ell''} \\ 0 \end{Bmatrix} \left[\frac{1}{r}\left(L_0^{\ell'} B^{U}_{0\,\ell'} + B^{V}_{0\,\ell'}\right) + \frac{dB^{V}_{0\,\ell'}}{dr} \right] \right.$$
$$\left. + \begin{Bmatrix} 0 \\ b^{U\,m}_{\ell'\,\ell''} \end{Bmatrix} \left(\frac{B^{W}_{0\,\ell'}}{r} + \frac{dB^{W}_{0\,\ell'}}{dr} \right) \right]$$
$$+ \begin{bmatrix} \ell & \ell' & \ell'' \\ 0 & + & + \\ m & 0 & m \end{bmatrix} \frac{L_0^{\ell''}}{r} \left[\begin{Bmatrix} b^{W\,m}_{\ell'\,\ell''} \\ 0 \end{Bmatrix} B^{W}_{0\,\ell'} + \begin{Bmatrix} 0 \\ b^{W\,m}_{\ell'\,\ell''} \end{Bmatrix} B^{V}_{0\,\ell'} \right] \tag{2.34}$$

and

$$-\mu_0\delta f^{W\,m}_{\ell} = \sum_{\ell'=0}^{\infty}\sum_{\ell''=|\ell-\ell'|}^{\ell+\ell'} \begin{bmatrix} \ell & \ell' & \ell'' \\ + & 0 & + \\ m & 0 & m \end{bmatrix} \left[\begin{Bmatrix} \frac{b^{W\,m}_{\ell'\,\ell''}}{r} + \frac{db^{W\,m}_{\ell'\,\ell''}}{dr} \\ \frac{1}{r}\left(L_0^{\ell''} b^{U\,m}_{\ell'\,\ell''} + b^{V\,m}_{\ell'\,\ell''}\right) + \frac{db^{V\,m}_{\ell'\,\ell''}}{dr} \end{Bmatrix} B^{U}_{0\,\ell'} + \begin{Bmatrix} b^{V\,m}_{\ell'\,\ell''} \\ b^{W\,m}_{\ell'\,\ell''} \end{Bmatrix} \frac{L_0^{\ell'}}{r} B^{W}_{0\,\ell'} \right]$$
$$+ \begin{bmatrix} \ell & \ell' & \ell'' \\ + & + & 0 \\ m & 0 & m \end{bmatrix} \left[\begin{Bmatrix} 0 \\ b^{U\,m}_{\ell'\,\ell''} \end{Bmatrix} \left[\frac{1}{r}\left(L_0^{\ell'} B^{U}_{0\,\ell'} + B^{V}_{0\,\ell'}\right) + \frac{dB^{V}_{\ell'}}{dr} \right] \right.$$
$$\left. + \begin{Bmatrix} b^{U\,m}_{\ell'\,\ell''} \\ 0 \end{Bmatrix} \left(\frac{B^{W}_{0\,\ell'}}{r} + \frac{dB^{W}_{0\,\ell'}}{dr} \right) \right]$$
$$+ \begin{bmatrix} \ell & \ell' & \ell'' \\ 0 & + & + \\ m & 0 & m \end{bmatrix} \frac{L_0^{\ell''}}{r} \left[\begin{Bmatrix} 0 \\ b^{W\,m}_{\ell'\,\ell''} \end{Bmatrix} B^{W}_{0\,\ell'} + \begin{Bmatrix} b^{W\,m}_{\ell'\,\ell''} \\ 0 \end{Bmatrix} B^{V}_{0\,\ell'} \right]. \tag{2.35}$$

Moreover, since $\mathbf{b}$ is divergence free, we have

$$\frac{db^{U\,m}_{\ell}}{dr} + \frac{1}{r}\left(2b^{U\,m}_{\ell} - L_0^{\ell} b^{V\,m}_{\ell}\right) = 0. \tag{2.36}$$

Finally, the relations between the poloidal scalar b^P and the spheroidal scalars b^U and b^V give

$$b^{U\,m}_{\ell} = L_0^{\ell} b^{P\,m}_{\ell} \tag{2.37}$$

and

$$b^{V^m}_{\ \ell} = \frac{db^{P^m}_{\ \ell}}{dr} + 2\frac{b^{P^m}_{\ \ell}}{r}. \tag{2.38}$$

2.4.5 Truncation of the displacement field and magnetic perturbation

Approximation or hypothesis 11

Our main interest is in the rotational modes of the Earth. In order to consider first the following truncated coupling chains

$$\mathbf{s} = \boldsymbol{\tau}^m_{\ell-1} + \boldsymbol{\sigma}^m_{\ell} + \boldsymbol{\tau}^m_{\ell+1} \tag{2.39}$$

and

$$\mathbf{b} = \mathbf{b}^{\tau m}_{\ell-1} + \mathbf{b}^{\sigma m}_{\ell} + \mathbf{b}^{\tau m}_{\ell+1}, \tag{2.40}$$

we make the

Approximation or hypothesis 12

The magnetic induction is spheroidal of odd degree or toroidal of even degree.
This implies that we consider 4 harmonic components for both $\mathbf{s}$ and $\mathbf{b}$. Of the 4 harmonic components for $\mathbf{b}$, only 3 are independent. Let us define the 4-dimensional vectors

$$y^s = (U^m_\ell,\ V^m_\ell,\ W^m_{\ell-1},\ W^m_{\ell+1})^T, \tag{2.41}$$

$$y^b = (b^{U^m}_{\ \ell},\ b^{V^m}_{\ \ell},\ b^{W^m}_{\ \ell-1},\ b^{W^m}_{\ \ell+1})^T \tag{2.42}$$

and

$$y^f = (\delta f^{U^m}_{\ \ell},\ \delta f^{V^m}_{\ \ell},\ \delta f^{W^m}_{\ \ell-1},\ \delta f^{W^m}_{\ \ell+1})^T. \tag{2.43}$$

2.4.6 Scalar equations of motion

Relations (2.27)-(2.30) and (2.33)-(2.35) can then be written

$$y^b = \mathcal{B}^1 y^s + \mathcal{B}^2 \frac{d}{dr} y^s \tag{2.44}$$

and

$$y^f = \mathcal{F}^1 y^b + \mathcal{F}^2 \frac{d}{dr} y^b, \tag{2.45}$$

where $\mathcal{B}^1$, $\mathcal{B}^2$, $\mathcal{F}^1$ and $\mathcal{F}^2$ are 4×4 matrices depending on $\mathbf{B}$ only. The relationship between the perturbation of the Lorentz force and $\mathbf{s}$ is

$$\begin{aligned} y^f &= \left(\mathcal{F}^1\mathcal{B}^1 + \mathcal{F}^2\frac{d}{dr}\mathcal{B}^1\right) y^s + \left(\mathcal{F}^1\mathcal{B}^2 + \mathcal{F}^2\mathcal{B}^1 + \mathcal{F}^2\frac{d}{dr}\mathcal{B}^2\right)\frac{d}{dr}y^s + \mathcal{F}^2\mathcal{B}^2\frac{d^2}{dr^2}y^s \\ &= \mathcal{M}^1 y^s + \mathcal{M}^2\frac{d}{dr}y^s + \mathcal{M}^3\frac{d^2}{dr^2}y^s. \end{aligned} \tag{2.46}$$

In the equations of motion, these terms introduce second derivatives of y^s. Before we took the Lorentz force into account, our system of ordinary differential equations was, however, designed in such a way that it only contained first derivatives of y^s and of the harmonic components of the normal stress : the stress-strain constitutive relationship provided a set of first-order ODEs for y^s and the equation of conservation of linear momentum provided a set of first-order ODEs for the components of the normal stress.

Solid inner core

In a solid layer, when we neglected the magnetic effects, the system of ODEs was written

$$\frac{d}{dr}y = \mathcal{A}y, \tag{2.47}$$

where $y = (U_\ell^m,\ P_\ell^m,\ \phi_\ell^m,\ g_\ell^m,\ V_\ell^m,\ W_{\ell-1}^m,\ W_{\ell+1}^m,\ Q_\ell^m,\ R_{\ell-1}^m,\ R_{\ell+1}^m)^T$. Now, by adding the Lorentz force, we obtain explicitly

$$\frac{d}{dr}y_i = \mathcal{A}_{ij}y_j \qquad i = 1,\ 3,\ 4,\ 5,\ 6,\ 7, \tag{2.48}$$

$$\frac{d}{dr}y_2 = \mathcal{A}_{2j}y_j + \mathcal{F}^1{}_{1k}y^b{}_k + \mathcal{F}^2{}_{1k}\frac{d}{dr}y^b{}_k, \tag{2.49}$$

$$\frac{d}{dr}y_i = \mathcal{A}_{ij}y_j + \mathcal{F}^1{}_{(i-6)k}y^b{}_k + \mathcal{F}^2{}_{(i-6)k}\frac{d}{dr}y^b{}_k \qquad i = 8,\ 9,\ 10, \tag{2.50}$$

$$y^b{}_i = \mathcal{B}^1{}_{ik}y^s{}_k + \mathcal{B}^2{}_{ik}\frac{d}{dr}y^s{}_k \qquad i = 1,\ 2,\ 3,\ 4, \tag{2.51}$$

the sums over j (from 1 to 10) and k (from 1 to 4) being implicit. If we define the vector $z = (y^T\ \ y^{bT})^T$, we have

$$\mathcal{B}^z\frac{d}{dr}z = \mathcal{A}^z z, \tag{2.52}$$

the lines of $\mathcal{B}^z$ and $\mathcal{A}^z$ being given by

$$\mathcal{B}^z{}_i = \begin{pmatrix} \mathcal{I}_i & 0 \end{pmatrix} \qquad i = 1,\ 3,\ 4,\ 5,\ 6,\ 7, \tag{2.53}$$

$$\mathcal{B}^z{}_2 = \begin{pmatrix} \mathcal{I}_2 & -\mathcal{F}^2{}_1 \end{pmatrix} \tag{2.54}$$

$$\mathcal{B}^z{}_i = \begin{pmatrix} \mathcal{I}_i & -\mathcal{F}^2{}_{i-6} \end{pmatrix} \qquad i = 8,\ 9,\ 10, \tag{2.55}$$

$$\mathcal{B}^z{}_i = \begin{pmatrix} -\mathcal{B}^2{}_{(i-10)1} & 0 & -\mathcal{B}^2{}_{(i-10)(2,3,4)} & 0 \end{pmatrix} \qquad i = 11,\ 12,\ 13,\ 14, \tag{2.56}$$

$$\mathcal{A}^z{}_i = \begin{pmatrix} \mathcal{A}_i & 0 \end{pmatrix} \qquad i = 1,\ 3,\ 4,\ 5,\ 6,\ 7, \tag{2.57}$$

$$\mathcal{A}^z{}_2 = \begin{pmatrix} \mathcal{A}_2 & \mathcal{F}^1{}_1 \end{pmatrix} \tag{2.58}$$

$$\mathcal{A}^z{}_i = \begin{pmatrix} \mathcal{A}_i & \mathcal{F}^1{}_{i-6} \end{pmatrix} \qquad i = 8,\ 9,\ 10, \tag{2.59}$$

$$\mathcal{A}^z{}_i = \begin{pmatrix} \mathcal{B}^1{}_{(i-10)1} & 0 & \mathcal{B}^1{}_{(i-10)(2,3,4)} & 0 & \mathcal{I}_i \end{pmatrix} \qquad i = 11,\ 12,\ 13,\ 14. \tag{2.60}$$

Liquid outer core

When we neglected the Lorentz force in the fluid outer core, the tangential components of the normal stress vanished and there were no differential equation either for V_ℓ^m or W_ℓ^m. Instead, they were both given by algebraic equations. Our system of equations in the fluid outer core was

$$\frac{d}{dr}y = \mathcal{A}^1 y + \mathcal{A}^2 x + \mathcal{A}^3 \frac{d}{dr}x \tag{2.61}$$

and

$$\mathcal{D}x = \mathcal{E}y, \tag{2.62}$$

where $y = (U_\ell^m,\ P_\ell^m,\ \phi_\ell^m,\ g_\ell^m)^T$ and $x = (V_\ell^m,\ W_{\ell-1}^m,\ W_{\ell+1}^m)^T$. Consequently,

$$\frac{d}{dr}y = \mathcal{A}y, \tag{2.63}$$

with

$$\mathcal{A} = (\mathcal{I} - \mathcal{A}^3\mathcal{D}^{-1}\mathcal{E})^{-1}\left\{\mathcal{A}^1 + \mathcal{A}^2\mathcal{D}^{-1}\mathcal{E} + \mathcal{A}^3\mathcal{D}^{-1}\left[\frac{d}{dr}\mathcal{E} - \left(\frac{d}{dr}\mathcal{D}\right)\mathcal{D}^{-1}\mathcal{E}\right]\right\}. \tag{2.64}$$

Now, by adding the Lorentz force, we obtain explicitly

$$\frac{d}{dr}y_i = \mathcal{A}^1{}_{ij}y_j + \mathcal{A}^2{}_{ik}x_k + \mathcal{A}^3{}_{ik}\frac{d}{dr}x_k \qquad i = 1,\ 3,\ 4, \tag{2.65}$$

$$\frac{d}{dr}y_2 = \mathcal{A}^1{}_{2j}y_j + \mathcal{A}^2{}_{2k}x_k + \mathcal{A}^3{}_{2k}\frac{d}{dr}x_k + \mathcal{F}^1{}_{1j}y^b{}_j + \mathcal{F}^2{}_{1j}\frac{d}{dr}y^b{}_j, \tag{2.66}$$

$$\mathcal{D}_{ik}x_k = \mathcal{E}_{ij}y_j + \mathcal{F}^1{}_{(i+1)j}y^b{}_j + \mathcal{F}^2{}_{(i+1)j}\frac{d}{dr}y^b{}_j \qquad i = 1,\ 2,\ 3, \tag{2.67}$$

$$y^b{}_i = \mathcal{B}^1{}_{ij}y^s{}_j + \mathcal{B}^2{}_{ij}\frac{d}{dr}y^s{}_j \qquad i = 1,\ 2,\ 3,\ 4, \tag{2.68}$$

the sums over j (from 1 to 4) and k (from 1 to 3) being implicit. If we define the vector $z = (y^T \quad x^T \quad y^{bT})^T = (U_\ell^m,\ P_\ell^m,\ \phi_\ell^m,\ g_\ell^m,\ V_\ell^m,\ W_{\ell-1}^m,\ W_{\ell+1}^m,\ b^{U^m}_{\ell},\ b^{V^m}_{\ell},\ b^{W^m}_{\ell-1},\ b^{W^m}_{\ell+1})^T$, we can write this system as

$$\mathcal{B}^z\frac{d}{dr}z = \mathcal{A}^z z, \tag{2.69}$$

where

$$\mathcal{B}^z{}_i = \begin{pmatrix} \mathcal{I}_i & -\mathcal{A}^3{}_i & 0 \end{pmatrix} \qquad i = 1,\ 3,\ 4, \tag{2.70}$$

$$\mathcal{B}^z{}_2 = \begin{pmatrix} \mathcal{I}_2 & -\mathcal{A}^3{}_2 & -\mathcal{F}^2{}_1 \end{pmatrix} \tag{2.71}$$

$$\mathcal{B}^z{}_i = \begin{pmatrix} 0 & 0 & -\mathcal{F}^2{}_{i-3} \end{pmatrix} \qquad i = 5,\ 6,\ 7, \tag{2.72}$$

$$\mathcal{B}^z{}_i = \begin{pmatrix} -\mathcal{B}^2{}_{(i-7)1} & 0 & -\mathcal{B}^2{}_{(i-7)(2,3,4)} & 0 \end{pmatrix} \qquad i = 8,\ 9,\ 10,\ 11, \tag{2.73}$$

$$\mathcal{A}^z{}_i = \begin{pmatrix} \mathcal{A}^1{}_i & \mathcal{A}^2{}_i & 0 \end{pmatrix} \qquad i = 1,\ 3,\ 4, \tag{2.74}$$

$$\mathcal{A}^z{}_2 = \begin{pmatrix} \mathcal{A}^1{}_2 & \mathcal{A}^2{}_2 & \mathcal{F}^1{}_1 \end{pmatrix} \tag{2.75}$$

$$\mathcal{A}^z{}_i = \begin{pmatrix} \mathcal{E}_{i-4} & -\mathcal{D}_{i-4} & \mathcal{F}^1{}_{i-3} \end{pmatrix} \qquad i = 5,\ 6,\ 7, \tag{2.76}$$

$$\mathcal{A}^z{}_i = \begin{pmatrix} \mathcal{B}^1{}_{(i-7)1} & 0 & \mathcal{B}^1{}_{(i-7)(2,3,4)} & \mathcal{I}_i \end{pmatrix} \qquad i = 8,\ 9,\ 10,\ 11. \tag{2.77}$$

2.4.7 Splitting of seismic normal modes by magnetic field

In collaboration with Bernard Valette and Mickaël Delatre (2007), we used the preceding formulas, in conjunction with a variational principle, to estimate the splitting of the seismic normal modes by the magnetic field in an attempt to provide an alternate explanation to the anomalous splitting of some of those modes (Ritzwoller et al. 1986, Widmer et al. 1992). Tanimoto (1989) already considered a dipolar or quadrupolar toroidal magnetic field acting on the displacement field of the seismic modes through the Lorentz force in the bulk of the outer core. He concluded that a strong magnetic field at the CMB is required to explain the anomalous splitting of a few normal modes sensitive to the structure of the core, which is usually explained by seismic anisotropy in the inner core. Earlier, Crossley and Smylie (1975) had considered a quadrupolar toroidal magnetic field and a magnetic boundary layer at the CMB. They had showed that the attenuation by the magnetic field of core sensitive modes is very weak. Also considering a simple geometry for the magnetic field, i. e. a dipolar poloidal field, we extended Tanimoto's and Crossley and Smylie's calculations by including the effects of (i) the Lorentz force in the bulk of the inner core and (ii) magnetic boundary layers at both the ICB and CMB. Whereas the magnitude of the magnetic field at the CMB is generally believed to be about 0.5 mT, it could be up to 50 times larger at the ICB. By computing the shifts of the eigenfrequencies and quality factors for split modes, we concluded that a radial magnetic field of order 1 T at the CMB would be necessary to explain the anomalous split modes.

In the next chapter, we are going to consider another mechanism for the splitting of the seismic normal modes : the splitting by rotation and ellipticity.

Chapitre 3

Modélisation numérique

On ne dormirait pas si l'on songeait à tout ce qu'il y a sous nos talons.

Bouvard et Pécuchet, Gustave Flaubert

[...] the Earth stove to the molten core of her. Where for aught any man knows lies the locality of Hell.

Blood Meridian, Cormac McCarthy

L'art de se tenir à propos sur la défensive ne le cède point à celui de combattre avec succès. Les experts dans la défense doivent s'enfoncer jusqu'au centre de la Terre. Ceux, au contraire, qui veulent briller dans l'attaque doivent s'élever jusqu'au neuvième ciel. Pour se mettre en défense contre l'ennemi, il faut être caché dans le sein de la Terre, comme ces veines d'eau dont on ne sait pas la source, et dont on ne saurait trouver les sentiers. C'est ainsi que vous cacherez toutes vos démarches, et que vous serez impénétrable.

L'art de la guerre, Sun Tzu

The fourth and most difficult step on the road of confidence building is that of providing a convincing physical explanation of an oscillation, once we have full statistical confirmation for its existence.

Ghil et al. (2002)

Ayant écrit un code numérique de résolution des équations des petites déformations de modèles de Terre en rotation, je l'ai appliqué à plusieurs problèmes qui, essentiellement, se répartissent en deux groupes : le calcul des modes sismiques et celui des modes de rotation.

3.1 Éclatement des modes sismiques et modes de Slichter

3.1.1 Introduction

Comme la rotation de la Terre est lente et que son aplatissement est petit, l'éclatement des féquences propres sismiques est petit et habituellement calculé au moyen d'une méthode de perturbation appliquée aux fréquences dégénérées du modèle sphérique de référence. Par rapport à une méthode de perturbation, le calcul direct des modes sismiques du modèle en rotation correspondant présente un double avantage. D'une part, il fournit à la fois, et au même ordre d'approximation, les déplacements propres et les fréquences propres éclatées, ou multiplets, alors qu'une méthode de perturbation est itérative et fournit d'abord les multiplets au premier ordre qui sont utilisés pour déterminer les déplacements propres au premier ordre, qui sont ensuite utilisés pour calculer les multiplets au second ordre, etc. D'autre part, il permet de traiter tout aussi facilement le cas des fréquences dégénérées qui sont presqu'égales et qui se retrouvent fortement couplées par la rotation et l'aplatissement, alors qu'une méthode de perturbation doit être spécialement adaptée à ce cas. Le code numérique sus-mentionné a été validé en comparant les résultats obtenus avec une méthode de perturbation des fréquences dégénérées et ceux obtenus par calcul direct des modes sismiques d'un modèle de Terre en rotation (Rogister 2003, Section 3.1.4). De plus, ces calculs ont permis de pointer l'ambigüité de l'identification, dans les observations sismologiques, des modes sismiques de fréquences proches.

Les modes de Slichter sont trois modes sismiques de translation quasi-rigide de la graine dans le noyau fluide. Leurs périodes, qui sont de quelques heures pour les modèles de Terre les plus réalistes, dépendent principalement de la différence entre la densité du noyau fluide à la frontière graine-noyau et la densité moyenne de la graine. L'observation dans les données de gravimètres supraconducteurs ainsi que la modélisation des modes de Slichter sont controversées depuis le début des années 1990. Le calcul des modes de Slichter décrit dans (Rogister 2003) indique que les études rapportant l'observation des modes de Slichter sont basées sur des approches théoriques inadéquates.

3.1.2 Splitting of the frequency of oscillation of a particle attached to a linear spring [1]

To illustrate the splitting of the eigenfrequencies of a mechanical system by rotation, we consider a simple example : a particle subjected only to the restoring force of a linear spring, the equilibrium position of the particle being fixed in absolute space. The particle is not constrained to move on a given curve or surface, so it has three degrees of freedom.

Viewed from an absolute system of reference, the trajectory of the particle is an ellipse and its position-vector is a sine function of time with a frequency, often called the natural frequency of the

1. Travail réalisé à l'instigation de Luis Rivera (IPGS) et avec sa collaboration.

system, that depends on the spring constant and the mass of the particle. By choosing appropriate initial conditions, the trajectory becomes a straight line on which the particle sinusoidally oscillates.

Viewed from of a system of reference that has both a fixed origin and a fixed axis in absolute space and is rotating at a constant speed with respect to the absolute space, the motion along the axis of rotation is a sinusoidal oscillation at the natural frequency and the motion in a plane perpendicular to the rotation axis is made up of three oscillations with frequencies equal to the frequency of rotation and the sum and difference of the frequency of rotation and the natural frequency mentioned above. The three oscillations can be visualized by considering specific trajectories, themselves determined by particular initial conditions. First, suppose that the particle is at rest at its equilibrium position *in absolute space*. An observer rotating with the relative system of reference therefore sees that the particle is rotating on a circle at the frequency of rotation of the relative system of reference. Second and third, in the specific case when the trajectory *in absolute space* is a circle in the plane perpendicular to the rotation axis and centered on the rotation axis, which is possible if the equilibrium position of the particle is on the rotation axis, the trajectory *in the rotating system of reference* is the same circle. Depending on the relative sense of the absolute rotations of the relative system and the particle, the frequency of the relative rotation of the particle will be the sum or the difference of the natural frequency and absolute frequency of rotation of the system of reference. It will be the sum (resp. difference) if, *in absolute space*, the particle and the relative system of reference are rotating in opposite senses (resp. the same sense).

Therefore, in the rotating system of reference, the degenerate natural frequency is split into three frequencies : the natural frequency itself and the sum and difference of the natural frequency and the frequency of rotation. The fourth frequency observed in the rotating frame, which is the frequency of rotation, does not come from the natural frequency ; it stems from the rotation of the relative system of reference. In absolute space, the particle is only subjected to the restoring force of the spring, which is spherically symmetrical about the equilibrium position of the particle. There is no preferred direction and the frequency of oscillation is the same in all directions. The rotation of the system of reference breaks the symmetry of the total force applied to the particle by imposing fictitious, or apparent, inertia forces in the equation of motion. This raises the degeneracy of the eigenfrequency. The frequency of the oscillation along the axis of rotation is still the natural frequency because that axis is no affected by rotation.

This simple example is, however, not completely analogous to the free vibrations of the Earth, considered a linearly elastic continuum. Indeed, the Earth particles are subjected to elastic constraints due to the contact with neighboring particles, which of course rotate. A particle attached to a linear spring with a rotating equilibrium position therefore provides a better analogy. To differentiate between these simple analogies with non-rotating and rotating equilibrium positions, we call them the non-rotating spring and rotating spring, respectively.

Observed in an absolute system of reference, the motion of a particle attached to a rotating spring is made up of a free oscillation at the natural frequency and a forced oscillation at the frequency of rotation, with a resonance when the two frequencies are equal. In a system of reference rotating with the spring, the degenerate normal mode frequency is split into three different frequencies, as for the non-rotating spring. The motion does not include any oscillation at the frequency of rotation.

Now, let us write this with equations.

Systems of reference

We consider an absolute system of reference $\mathcal{S}$, with an origin O and axes X, Y, Z, and a relative system of reference $\mathfrak{S}$, with the same origin O, axes x, y, z and rotating at constant angular speed $\mathbf{\Omega} = \Omega\mathbf{e}_Z = \Omega\mathbf{e}_z$ about the $Z = z$ axis.

Kinematics

We denote by $\mathbf{R} = \mathbf{OP}$ the position-vector of a moving particle in $\mathcal{S}$ and by $\mathbf{r}$, the position-vector in $\mathfrak{S}$. Since $\mathcal{S}$ and $\mathfrak{S}$ have the same origin, the two vectors are actually equal but their components are different. We denote the components of $\mathbf{R}$ in $\mathcal{S}$ by $(X, Y, Z)_{\mathcal{S}}$, and the components of $\mathbf{r}$ in $\mathfrak{S}$ by $(x, y, z)_{\mathfrak{S}}$. If the $\mathcal{S}$ and $\mathfrak{S}$ coincide at $t = 0$, the components at time t are related by

$$x = X\cos\Omega t + Y\sin\Omega t \tag{3.1}$$
$$y = -X\sin\Omega t + Y\cos\Omega t \tag{3.2}$$
$$z = Z. \tag{3.3}$$

The velocities in $\mathcal{S}$ and $\mathfrak{S}$ are, respectively, $\mathbf{V} = \dot{\mathbf{R}}$ and $\mathbf{v} = \mathbf{r}'$, where the dot designates the time derivative in $\mathcal{S}$ and the prime designates the time derivative in $\mathfrak{S}$. According to Poisson's formula, we have

$$\mathbf{V} = \mathbf{v} + \mathbf{\Omega} \times \mathbf{r}. \tag{3.4}$$

We also define the accelerations in $\mathcal{S}$ and $\mathfrak{S}$ by $\mathbf{\Gamma} = \dot{\mathbf{V}}$ and $\boldsymbol{\gamma} = \mathbf{v}'$, respectively. The relation between the accelerations is

$$\mathbf{\Gamma} = \boldsymbol{\gamma} + 2\mathbf{\Omega} \times \mathbf{v} + \mathbf{\Omega} \times (\mathbf{\Omega} \times \mathbf{r}). \tag{3.5}$$

Non-rotating spring

We consider a particle of mass m attached to a linear spring, which means it is subjected to the restoring force $-k\mathbf{LP}$, where k is a constant and L is a fixed point on the X-axis such that $|\mathbf{OL}| = l$, which is Hooke's law. Denoting $\mathbf{LP}$ by $\mathbf{\Delta}$, the position P in $\mathcal{S}$ is given by

$$\mathbf{R} = l\mathbf{e}_X + \mathbf{\Delta} = (l + \Delta_X)\mathbf{e}_X + \Delta_Y\mathbf{e}_Y + \Delta_Z\mathbf{e}_Z \tag{3.6}$$

and the equation of motion is

$$m\mathbf{\Gamma} = -k\mathbf{\Delta}. \tag{3.7}$$

The motion is the solution of this equation. It is an oscillatory motion on an elliptical trajectory (see Section 3.1.3) :

$$X = l + A_1\cos\omega t + A_2\sin\omega t \tag{3.8}$$
$$Y = A_3\cos\omega t + A_4\sin\omega t \tag{3.9}$$
$$Z = A_5\cos\omega t + A_6\sin\omega t \tag{3.10}$$

where $\omega^2 = k/m$ and the A_is are constants that will be determined below by using the initial conditions.

Let us now consider the motion of P in $\mathfrak{S}$. Denoting $\mathbf{LP}$ by $\boldsymbol{\delta}$, the components of the position-vector are

$$\mathbf{r} = l(\cos\Omega t\,\mathbf{e}_x - \sin\Omega t\,\mathbf{e}_y) + \delta_x\mathbf{e}_x + \delta_y\mathbf{e}_y + \delta_z\mathbf{e}_z, \tag{3.11}$$

The equation of motion

$$m\boldsymbol{\gamma} = -k\boldsymbol{\delta} - 2m\boldsymbol{\Omega}\times\mathbf{v} - m\boldsymbol{\Omega}\times(\boldsymbol{\Omega}\times\mathbf{r}) \tag{3.12}$$

gives

$$\delta_x'' + (\omega^2 - \Omega^2)\delta_x - 2\Omega\delta_y' + \omega^2 l\cos\Omega t = 0 \tag{3.13}$$
$$\delta_y'' + (\omega^2 - \Omega^2)\delta_y + 2\Omega\delta_x' - \omega^2 l\sin\Omega t = 0 \tag{3.14}$$
$$\delta_z'' + \omega^2\delta_z = 0. \tag{3.15}$$

Let

$$u = \delta_x + i\delta_y. \tag{3.16}$$

u obeys the differential equation

$$u'' + 2i\Omega u' + (\omega^2 - \Omega^2)u + \omega^2 l e^{-i\Omega t} = 0, \tag{3.17}$$

from which we obtain

$$x = a_1\cos(\omega+\Omega)t + a_2\sin(\omega+\Omega)t + a_3\cos(\omega-\Omega)t + a_4\sin(\omega-\Omega)t + l\cos\Omega t \tag{3.18}$$
$$y = -a_1\sin(\omega+\Omega)t + a_2\cos(\omega+\Omega)t + a_3\sin(\omega-\Omega)t - a_4\cos(\omega-\Omega)t - l\sin\Omega t \tag{3.19}$$
$$z = a_5\cos\omega t + a_6\sin\omega t, \tag{3.20}$$

where the a_is are constants. An observer at O rotating with the system of reference $\mathfrak{S}$ therefore sees the motion of P as an oscillation of frequency ω along the z-axis and, in the xy plane, the superposition of three oscillations of frequencies $\omega-\Omega$, $\omega+\Omega$ and ω. The degeneracy of the motion observed in $\mathcal{S}$ is, in $\mathfrak{S}$, raised by the rotation of the system of reference $\mathfrak{S}$.

To simplify further, we suppose that L = O. Consequently, $l = 0$ and the motion in the xy plane is just the superposition of two normal modes of frequencies $\omega - \Omega$ and $\omega + \Omega$. The displacements associated to three normal modes clearly appear in the solution (3.18) – (3.20) : the first two are rotations about the z-axis and the third is a translation along the z-axis.

Rotating spring

We now consider a particle subjected to the restoring force $-k\mathbf{L}'\mathbf{P}$, where k is a constant and L' is a fixed point on x such that $|\mathbf{OL}'| = l$.

In $\mathcal{S}$, the position-vector is

$$\mathbf{R} = l(\cos\Omega t\,\mathbf{e}_X + \sin\Omega t\,\mathbf{e}_Y) + \boldsymbol{\Delta} \tag{3.21}$$

and the equation of motion (3.7) gives

$$\ddot{\Delta}_X + \omega^2 \Delta_X - \Omega^2 l \cos \Omega t = 0 \tag{3.22}$$

$$\ddot{\Delta}_Y + \omega^2 \Delta_Y - \Omega^2 l \sin \Omega t = 0 \tag{3.23}$$

$$\ddot{\Delta}_Z + \omega^2 \Delta_Z = 0. \tag{3.24}$$

The motion is therefore

$$X = A_1 \cos \omega t + A_2 \sin \omega t + \frac{l\omega^2}{\omega^2 - \Omega^2} \cos \Omega t \tag{3.25}$$

$$Y = A_3 \cos \omega t + A_4 \sin \omega t + \frac{l\omega^2}{\omega^2 - \Omega^2} \sin \Omega t \tag{3.26}$$

$$Z = A_5 \cos \omega t + A_6 \sin \omega t \tag{3.27}$$

In addition to the oscillation of frequency ω, the particle oscillates at the frequency Ω in the xy plane, which is of course due to the rotation of the spring. If $\omega = \Omega$, we recover the resonance phenomenon encountered when a system is forced to oscillate at one of its natural frequencies.

We turn to the description of the motion in $\mathfrak{S}$. The position-vector is

$$\mathbf{r} = l\mathbf{e}_x + \delta_x \mathbf{e}_x + \delta_y \mathbf{e}_y + \delta_z \mathbf{e}_z \tag{3.28}$$

and the projections of the equation of motion (3.12) on the three axes are

$$\delta_x'' + (\omega^2 - \Omega^2)\delta_x - 2\Omega\delta_y' - \Omega^2 l = 0 \tag{3.29}$$

$$\delta_y'' + (\omega^2 - \Omega^2)\delta_y + 2\Omega\delta_x' = 0 \tag{3.30}$$

$$\delta_z'' + \omega^2 \delta_z = 0. \tag{3.31}$$

The variable u defined by (3.16) obeys the differential equation

$$u'' + 2i\Omega u' + (\omega^2 - \Omega^2)u - \Omega^2 l = 0. \tag{3.32}$$

We then find the motion in $\mathfrak{S}$:

$$x = a_1 \cos(\omega + \Omega)t + a_2 \sin(\omega + \Omega)t + a_3 \cos(\omega - \Omega)t + a_4 \sin(\omega - \Omega)t + \frac{l\omega^2}{\omega^2 - \Omega^2} \tag{3.33}$$

$$y = -a_1 \sin(\omega + \Omega)t + a_2 \cos(\omega + \Omega)t + a_3 \sin(\omega - \Omega)t - a_4 \cos(\omega - \Omega)t \tag{3.34}$$

$$z = a_5 \cos \omega t + a_6 \sin \omega t \tag{3.35}$$

Obviously, we again find that the oscillation of frequency ω observed in $\mathcal{S}$ is split into two oscillations of frequencies $\omega - \Omega$ and $\omega + \Omega$. The displacements associated to the normal modes are as for the non-rotating spring, i.e. a translation along and rotations about the $z-$axis.

Because there is no relative motion of the spring with respect to the rotating system of reference $\mathfrak{S}$, the motion of P does not contain any oscillation of frequency Ω, contrary to the solutions (3.18)-(3.20).

Initial conditions

To simplify the solutions derived above, we consider specific initial conditions, first for the non-rotating spring, second for the rotating spring. In particular, we assume that there is no initial velocity along the $z = Z$-axis, so there is no motion along that axis.

Non-rotating spring In $\mathcal{S}$, we set $X(0) = X_0$, $\dot{X}(0) = 0$, $Y(0) = 0$, $\dot{Y}(0) = \dot{Y}_0$, $Z(0) = 0$, and $\dot{Z}(0) = 0$. The solution then reads

$$X = l + (X_0 - l)\cos\omega t \tag{3.36}$$
$$Y = \frac{\dot{Y}_0}{\omega}\sin\omega t \tag{3.37}$$
$$Z = 0. \tag{3.38}$$

The trajectory is an ellipse centered at $(l,\, 0,\, 0)$ with semi-axes $X_0 - l$ and $\dot{Y}_0/\omega$.

In $\mathfrak{S}$, the same initial conditions together with Eqs (3.1)-(3.4) give $x(0) = x_0 = X_0$, $y(0) = y_0 = Y_0$, $\dot{x}(0) = -\Omega y_0 = \dot{x}_0$, $\dot{y}(0) = \dot{Y}_0 + \Omega x_0 = \dot{y}_0$, $Z(0) = 0$, and $\dot{Z}(0) = 0$ Therefore, the a_i's $(i = 1 \ldots 6)$ are given by

$$a_1 = \frac{\omega - \Omega}{2\omega}x_0 - \frac{1}{2\omega}\dot{y}_0 - \frac{l}{2} \tag{3.39}$$
$$a_2 = \frac{\omega - \Omega}{2\omega}y_0 + \frac{1}{2\omega}\dot{x}_0 \tag{3.40}$$
$$a_3 = \frac{\omega + \Omega}{2\omega}x_0 + \frac{1}{2\omega}\dot{y}_0 - \frac{l}{2} \tag{3.41}$$
$$a_4 = -\frac{\omega + \Omega}{2\omega}y_0 + \frac{1}{2\omega}\dot{x}_0 \tag{3.42}$$
$$a_5 = a_6 = 0. \tag{3.43}$$

By choosing appropriate initial conditions, it is always possible to have either a_1 and a_2 or a_3 and a_4 both different from zero, therefore exciting only one of the two normal modes, as can be seen by inspection of (3.18) and (3.19). The eigendisplacements of the two modes are rotations about the $z-$axis.

Rotating spring Given the similarity of the solutions (3.8)-(3.10) and (3.25)-(3.27) in $\mathcal{S}$ and solutions (3.18)-(3.20) and (3.33)-(3.35) in $\mathfrak{S}$, we can readily write the a_i's as functions of the initial conditions for the rotating spring. For instance, if in $\mathfrak{S}$, we set $x(0) = x_0$, $x'(0) = x'_0$, $y(0) = y_0$, $y'(0) = y'_0$, $z(0) = 0$, and $z'(0) = 0$, we have

$$a_1 = \frac{\omega - \Omega}{2\omega}x_0 - \frac{1}{2\omega}y'_0 - \frac{\omega}{2(\omega + \Omega)}l \tag{3.44}$$
$$a_2 = \frac{\omega - \Omega}{2\omega}y_0 + \frac{1}{2\omega}x'_0 \tag{3.45}$$
$$a_3 = \frac{\omega + \Omega}{2\omega}x_0 + \frac{1}{2\omega}y'_0 - \frac{\omega}{2(\omega - \Omega)}l \tag{3.46}$$
$$a_4 = -\frac{\omega + \Omega}{2\omega}y_0 + \frac{1}{2\omega}x'_0 \tag{3.47}$$
$$a_5 = a_6 = 0. \tag{3.48}$$

and the same conclusions can be drawn for the rotating spring as for the non-rotating spring.

3.1.3 Elliptical trajectories of particles in inner core for the Slichter mode of a non-rotating spherical model

We consider a non-rotating spherical Earth model. Therefore, the spheroidal and toroidal deformations decouple. Moreover, deformations of different degrees and orders also decouple. The goal of this short section is to show that, for the Slichter mode, the trajectories of the particles in the inner core are ellipses.

The Slichter mode is the gravest degree-1 mode. Its is three times degenerate. A degree-1, order-0 spheroidal displacement writes

$$\boldsymbol{\sigma}_1^0(\mathbf{r}) = U_1^0(r)\cos\theta\,\mathbf{e}_r + \frac{1}{2}V_1^0(r)\sin\theta\,\mathbf{e}_\theta, \tag{3.49}$$

where r is the radius, $\mathbf{e}_r$ is the radial unit vector, θ is the colatitude and $\mathbf{e}_\theta$ is the tangent unit vector in a meridian plane. $\boldsymbol{\sigma}_1^0$, U_1^0 and V_1^0 also depend on the frequency of the oscillation. For the Slichter mode, numerical calculation gives, independently of the radial structure of the Earth model,

$$U_1^0 = -\frac{1}{2}V_1^0 \tag{3.50}$$

in the inner core. Moreover, U_1^0 and V_1^0 do not depend on r. Therefore,

$$\boldsymbol{\sigma}_1^0 = U_1^0\mathbf{e}_z, \tag{3.51}$$

in the inner core, $\mathbf{e}_z$ being the unit vector along the $z-$axis.

It is easy to show that the eigendisplacements of the Slichter modes of orders ±1 are

$$\boldsymbol{\sigma}_1^{\pm1} = U_1^{\pm1}(\mathbf{e}_x \pm i\mathbf{e}_y), \tag{3.52}$$

where $U_1^{\pm1}$ are constants. Because of the spherical symmetry and eigenfrequency degeneracy, the following vectors are also eigendisplacements of the Slichter mode :

$$\boldsymbol{\sigma}_1^x = U_1^x\mathbf{e}_x \tag{3.53}$$

and

$$\boldsymbol{\sigma}_1^y = U_1^y\mathbf{e}_y, \tag{3.54}$$

U_1^x and U_1^y being also constants. Since the inner core translates as a rigid body, it is sufficient to consider the motion of its center of mass C. We denote the Cartesian coordinates of its position by x_C, y_C, and z_C. Given an arbitrary excitation, the motion of C for the Slichter mode is the sum of three harmonic oscillations of frequency ω along the x, y, and z axes :

$$x_\mathrm{C} = x_0\cos\omega t + \frac{\dot{x}_0}{\omega}\sin\omega t, \tag{3.55}$$

$$y_\mathrm{C} = y_0\cos\omega t + \frac{\dot{y}_0}{\omega}\sin\omega t, \tag{3.56}$$

$$z_\mathrm{C} = y_0\cos\omega t + \frac{\dot{z}_0}{\omega}\sin\omega t, \tag{3.57}$$

where $\mathbf{r}_0 = (x_0,\, y_0,\, z_0)$ and $\mathbf{v}_0 = (\dot{x}_0,\, \dot{y}_0,\, \dot{z}_0)$ are, respectively, the initial position and initial velocity of C. $\mathbf{v}_0$ is determined by the excitation mechanism. The trajectory of C is obtained by eliminating t between (3.55), (3.56), and (3.57).

First, the trajectory is plane. Indeed, the cross product $\mathbf{r}_\mathrm{C} \times \mathbf{v}_\mathrm{C}$ is a constant vector. Therefore, both $\mathbf{r}_\mathrm{C}$ and $\mathbf{v}_\mathrm{C}$ are perpendicular to a constant direction or, equivalently, are in the same plane.

Second, the trajectory is a closed curve because, after times $T = 2\pi n/\omega$ (n integer), C returns to its initial position.

Third, the trajectory is an ellipse. Indeed, it is possible to orientate the axes of a system of reference $\mathrm{O}\mathcal{X}\mathcal{Y}\mathcal{Z}$ in such a way that the motion takes place in a plane perpendicular to the $\mathcal{Z}$ axis. Consequently, the coordinates $\mathcal{X}_\mathrm{C}$ and $\mathcal{Y}_\mathrm{C}$ of the centre of mass are

$$\mathcal{X}_\mathrm{C} = \mathcal{X}_0 \cos\omega t + \frac{\dot{\mathcal{X}}_0}{\omega} \sin\omega t, \tag{3.58}$$

$$\mathcal{Y}_\mathrm{C} = \mathcal{Y}_0 \cos\omega t + \frac{\dot{\mathcal{Y}}_0}{\omega} \sin\omega t. \tag{3.59}$$

It is next possible to orientate the $\mathcal{X}$ and $\mathcal{Y}$ axes so that $\dot{\mathcal{X}}_0 = 0$. The equation of the trajectory is thus given by

$$\mathcal{Y}^2 + \frac{1}{\mathcal{X}_0^2}\left(\mathcal{Y}2_0 + \frac{\dot{\mathcal{Y}}_0^2}{\omega^2}\right)\mathcal{X}^2 - 2\frac{\mathcal{Y}_0}{\mathcal{X}_0}\mathcal{X}\mathcal{Y} = \frac{\dot{\mathcal{Y}}_0^2}{\omega^2}, \tag{3.60}$$

which is the equation of an ellipse.

Rotation and ellipticity make things slightly more complicated. In that case, the trajectories of the particles are nicely illustrated by Smith (1976).

3.1.4 *Splitting of seismic free oscillations and of the Slichter triplet using the normal mode theory of a rotating, ellipsoidal earth*

This paper was published in 2003 in Physics of the Earth and planetary Interiors (**140**, 169–182).

3.2 Influence de la structure du noyau liquide sur les modes de rotation

3.2.1 Introduction

Lorsqu'on néglige le champ magnétique, qui est généré dans le noyau liquide, et la viscosité de ce dernier, le spectre associé au noyau dépend de deux paramètres : la vitesse de rotation et la stratification thermique, qui est quantifiée sous la forme de la fréquence de Brunt-Väisälä. Valette (1989a, b) a montré que le spectre est continu et a déterminé ses bornes. Les modes de rotation, immergés dans le spectre du noyau, sont influencés par lui, voire fortement influencés lorsqu'il s'agit des modes de rotation du noyau et de la graine. La méthode de calcul des déformations gravito-élastiques évoquée plus haut repose sur la décomposition du champ des déplacements en une série d'harmoniques sphériques et sur une troncature de cette série, bien que les termes soient tous

couplés. Des modes dont l'énergie est localisée dans le noyau ressortent des solutions numériques. Parmi eux, nous retrouvons les modes planétaires, ou modes de Rossby, bien connus par ailleurs. L'existence des autres modes n'est confirmée par aucune autre théorie ni aucune observation. Ceci nous incite à les qualifier de pseudo-modes.

En faisant varier la stratification thermique du noyau dans les limites permises par la sismologie, nous avons montré que les modes de rotation et des pseudo-modes du noyau interagissent lorsque leurs fréquences sont voisines. Ainsi, le mouvement de Chandler s'en trouve dédoublé (Rogister et Valette 2005, Section 3.2.2), comme le suggèrent d'ailleurs de nombreuses analyses des données du mouvement du pôle. Les périodes des deux oscillations ne sont jamais égales mais sont séparées de quelques jours au moins. Ce phénomène se manifeste aussi pour la nutation libre du noyau et la nutation libre de la graine (Rogister et Valette 2009, Section 3.2.3). L'effet sur la nutation libre du noyau est faible, les deux périodes restant proches de 430 jours - dans un repère absolu - et séparées de quelques jours. Par contre, l'effet sur la nutation libre de la graine est très important : la différence des deux périodes propres va jusqu'à plusieurs centaines de jours, toujours dans un repère absolu.

Le cas du mouvement de Chandler de la graine est encore différent. Par exemple, un modèle simple de Terre, constitué d'une graine et d'un manteau rigides et d'un noyau incompressible, possède une famille de modes dont les mouvements propres sont dominés par un mouvement du pôle de la graine et des oscillations dans le noyau fluide. Le mouvement du pôle de la graine est son mouvement de Chandler qui, ici, est donc multiple (Rogister 2010, Section 3.2.4).

3.2.2 *Influence of outer core dynamics on Chandler wobble*

This paper, written with Bernard Valette, was published in 2005 in *Forcing of Polar Motion in the Chandler Frequency Band : A Contribution to Understanding Interannual Climate Variations*, éds H.-P. Plag et al., Cahiers du Centre Européen de Géodynamique et de Séismologie (**24**, 61–68), Walferdange, Luxembourg.

3.2.3 *Influence of liquid core dynamics on rotational modes*

This paper, also written with Bernard Valette, was published in 2009 in Geophysical Journal International (**176**, 368–388).

3.2.4 *Multiple inner core wobble in a simple Earth model with inviscid core*

This paper was published in 2010 in Physics of the Earth and planetary Interiors (**178**, 8–15).

Chapitre 4

Comparaison entre modélisations de la rotation terrestre

4.1 Motivation

Le domaine scientifique qui devrait être le plus concerné par les résultats décrits au chapitre précédent est la géodésie, en particulier l'étude de la rotation terrestre. Toutefois, les communiquer à la communauté des géodésiens s'est souvent révélé difficile, pour deux raisons, me semble-t-il. La première est que, pour modéliser les variations de la rotation terrestre, les méthodes de calcul exposées au Chapitre 2, basées sur une résolution numérique des équations locales de conservation de la quantité de mouvement, ne sont pas communément utilisées. Une méthode basée sur les équations dites de Liouville est beaucoup plus familière à bon nombre de géodésiens. D'ailleurs, elle est à la base du modèle de référence de nutation-précession adopté par l'Union Astronomique Internationale en 2003. Telle qu'elle est implémentée, elle néglige la dynamique du noyau liquide, ce qui peut être la source de la seconde raison qui explique la difficulté de communiquer les résultats du Chapitre 3 : l'interaction entre le spectre du noyau et les modes de rotation n'est pas un sujet d'étude répandu.

La dernière partie de ce travail vise donc d'abord à comparer et relier les théories des modes de rotation (ce chapitre), et ensuite à établir des analogies avec d'autres domaines de la géophysique, ou même avec la physique, où des interactions entre modes normaux sont fréquentes (Chapitre 5).

4.2 Introduction

Les études théoriques des nutations terrestres reposent généralement sur l'une des deux approches suivantes : (i) l'approche locale qui consiste à résoudre les équations locales de l'élasto-gravité ou (ii) l'approche globale qui consiste à résoudre les équations de conservation des moments cinétiques de la graine, du noyau liquide et du manteau, connaissant les couples de forces qui agissent aux interfaces et en surface. La première méthode, qui est celle utilisée par les sismologues pour étudier les déformations de la Terre, a fourni un modèle de nutations qui a été le modèle de référence de l'Union Astronomique Internationale entre 1980 et 2002. Le modèle MHB2000 adopté par l'UAI depuis 2003 est basé sur la seconde méthode, qui est davantage utilisée par les géodésiens

et les astronomes.

La présentation consiste en une comparaison des deux approches en insistant sur les hypothèses et les approximations qui les caractérisent.

4.3 1980 and 2000 IAU Theories of Nutation

Among the resolutions adopted at the 24th General Assembly of the International Astronomical Union held in Manchester in August 2000, Resolution B1.6 recommends that

> beginning on 1 January 2003, the IAU 1976 Precession Model and IAU 1980 Theory of Nutation, be replaced by the precession-nutation model IAU 2000A (MHB2000, based on the transfer functions of Mathews, Herring and Buffett, 2000 - submitted to the Journal of Geophysical Research) for those who need a model at the 0.2 mas level, or its shorter version IAU 2000B for those who need a model only at the 1 mas level, together with their associated precession and obliquity rates, and their associated celestial pole offsets at J2000, to be published in the IERS Conventions 2000.

The actual references for the 1980 IAU Theory of Nutation and nutation series MHB2000 are Seidelmann (1982) and Mathews et al. (2002), respectively. The purpose of this paper is to compare the theoretical approaches to the nutations of a deformable Earth on which the models IAU 1980 and IAU 2000 are based. Actually, the nutation models also rely on the calculation of the nutations of a rigid Earth, the amplitude of a nutation of a deformable Earth in the frequency domain being given by the product of the nutation amplitude of the corresponding rigid model with the transfer functions of the deformable model. Models IAU 1980 and IAU 2000 are based on different rigid Earth nutation series. However, since we will not deal with the nutations of a rigid Earth, we can without ambiguity distinguish the theoretical approaches to the nutations, or equivalently to the transfer functions, of a deformable Earth by calling them according to the name of the IAU nutation model they are part of.

The computation of the nutations of a deformable rotating Earth involves three major steps :

1. Writing of the fundamental equations of continuum mechanics in a given system of reference,
2. Description of the physical properties and behaviour of the Earth's model through constitutive equations,
3. Resolution of the field equations written in the first two steps supplemented with appropriate boundary conditions.

Each step is different for models IAU 1980 and IAU 2000. Notably, step 2 is more sophisticated for model IAU 2000. But, in principle, the IAU 1980 model can be adapted to manage the same refinements as the IAU 2000 model. Our comparison will focus on steps 1 and 3. To make it meaningful, it is necessary to consider the same Earth's model and physical phenomena for the two approaches, namely step 2 must be the same. Therefore, as in model IAU 1980, we will consider an elliptical, rotating, hydrostatically prestressed Earth model with an isotropic elastic stress-strain relationship. We will neglect the anelastic, electromagnetic, and ocean tide effects that are taken into account in model IAU 2000.

Step 1, described in Section 4.4, consists in writing, in a rotating system of reference, the linearized equation of conservation of linear momentum, Poisson's equation for the variation of

gravity potential, the stress-strain relationship, and the continuity and boundary conditions. Step 1 is similar for both the IAU 1980 and IAU 2000 models, except that the systems of reference are different.

In step 3, the displacement is split into spheroidal and toroidal fields, then each part is expanded in series of spherical harmonics, as is the variation of the gravity potential. From there on, the resolution methods diverge. In model IAU 1980, the equations of motion are directly solved, most of the time numerically, after truncature of the series describing the displacement field and variation of the gravity potential. In model IAU 2000, the wobbles of the different layers (mantle, outer core, inner core) are obtained by solving the Euler-Liouville equations for the conservation of the total absolute angular momenta of the layers, whereas the deformational part of the displacement field is approximated by the deformation of the corresponding non-rotating spherical model submitted to a variable centripetal force. We describe step 3 in Section 4.5. Of course, we will not rederive all the details of the two approaches. We will refer the reader to the original papers where they are exposed.

In the following, we will often split the page into two columns to facilitate the comparison between the two methods. The IAU 1980 (resp. 2000) model will be described in the left (resp. right) column. Alternatively, we will call the IAU 1980 model, the Linear Momentum (LM) approach, and the IAU 2000 model, the Angular Momentum (AM) approach.

4.4 Systems of reference and equations of motion

Let us start with the first step of the program established on page 30. The two approaches use different systems of reference, which we shall denote by $\mathfrak{S}$ and $\mathfrak{s}$ and define as follows.

IAU 1980 - LM

The X and Y axes of the reference frame $\mathfrak{S}$ steadily rotate at a constant speed $\mathbf{\Omega}_0$ about the Z axis, which is fixed with respect to an inertial frame.

IAU 2000 - AM

The x, y and z axes of the reference frame $\mathfrak{s}$ rotate at a variable absolute speed $\mathbf{\Omega}$ defined below by Eqs (4.23) and (4.25).

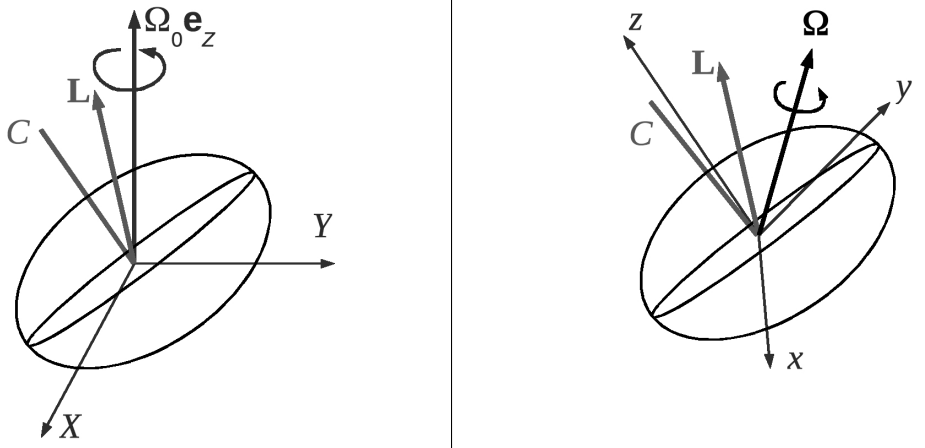

FIGURE 4.1 – Ellipsoidal Earth and systems of reference $\mathfrak{S}$ (left) and $\mathfrak{s}$ (right). $\mathbf{\Omega}_0$ (resp. $\mathbf{\Omega}$) is the constant (resp. variable) absolute velocity of rotation of $\mathfrak{S}$ (reps. $\mathfrak{s}$). $\mathbf{L}$ is the total absolute angular momentum of the Earth and C designates the unperturbed polar moment of inertia.

We will denote the time, density, displacement field, Lagrangean variation of the Cauchy stress tensor, unperturbed gravitational potential and gravity potential, Eulerian variation of the gravity potential and external forces by

T, ρ, $\mathbf{S}$, $\delta\boldsymbol{T}$, ϕ, $\tilde{\Phi}$, Φ' and $\mathbf{f}$, | t, ρ, $\mathbf{s}$, $\delta\boldsymbol{t}$, ϕ, $\tilde{\phi}$, ϕ' and $\mathbf{f}$,

respectively.

In $\mathfrak{S}$ and $\mathfrak{s}$, the linearized equations of motion write

$$\rho\frac{d^2\mathbf{S}}{dT^2} = \boldsymbol{\nabla}\cdot\delta\boldsymbol{T} - \rho\boldsymbol{\nabla}\Phi' + \rho\left(\boldsymbol{\nabla}\cdot\mathbf{S}\right)\boldsymbol{\nabla}\tilde{\Phi} - \rho\boldsymbol{\nabla}\left(\mathbf{S}\cdot\boldsymbol{\nabla}\tilde{\Phi}\right) - 2\rho\mathbf{\Omega}_0\times\frac{d\mathbf{S}}{dT} + \mathbf{f} \tag{4.1}$$

$$\tilde{\Phi} = \phi - \frac{1}{2}|\mathbf{\Omega}_0\times\mathbf{r}|^2 \tag{4.2}$$

$$\nabla^2\Phi' = -4\pi\mathrm{G}\,\boldsymbol{\nabla}\cdot\rho\mathbf{S} \tag{4.3}$$

$$\rho\frac{d^2\mathbf{s}}{dt^2} = \boldsymbol{\nabla}\cdot\delta\boldsymbol{t} - \rho\boldsymbol{\nabla}\phi' + \rho\left(\boldsymbol{\nabla}\cdot\mathbf{s}\right)\boldsymbol{\nabla}\tilde{\phi} - \rho\boldsymbol{\nabla}\left(\mathbf{s}\cdot\boldsymbol{\nabla}\tilde{\phi}\right) - 2\rho\mathbf{\Omega}\times\frac{d\mathbf{s}}{dt} - \rho\frac{d\mathbf{\Omega}}{dt}\times\mathbf{r} + \mathbf{f} \tag{4.4}$$

$$\tilde{\phi} = \phi - \frac{1}{2}|\mathbf{\Omega}\times\mathbf{r}|^2 \tag{4.5}$$

$$\nabla^2\phi' = -4\pi\mathrm{G}\,\boldsymbol{\nabla}\cdot\rho\mathbf{s} \tag{4.6}$$

The unperturbed gravitational potential

$$\phi\left(\mathbf{r}\right) = -\mathrm{G}\int_{\mathcal{V}}\frac{\rho}{|\mathbf{r}-\mathbf{r}'|}\,d\mathcal{V}', \tag{4.7}$$

where $\mathcal{V}$ is the unperturbed Earth, is a solution of Poisson's equation

$$\nabla^2\phi = 4\pi \mathrm{G}\rho. \tag{4.8}$$

The velocities $d\mathbf{S}/dt$ in $\mathfrak{S}$ and $d\mathbf{s}/dt$ in $\mathfrak{s}$ of a particle at $\mathbf{r}$ are related by

$$\frac{d\mathbf{S}}{dT} = (\boldsymbol{\Omega} - \boldsymbol{\Omega}_0) \times \mathbf{r} + \frac{d\mathbf{s}}{dt}, \tag{4.9}$$

where $\boldsymbol{\Omega} - \boldsymbol{\Omega}_0$ is the speed of rotation of $\mathfrak{s}$ with respect to $\mathfrak{S}$.

A stress-strain relationship must be added to describe the rheological behaviour of the Earth (Step 2 of the program on page 30). For an isotropic elastic material, we have

$$\delta\boldsymbol{T} = \lambda(\boldsymbol{\nabla}\cdot\mathbf{S})\,\boldsymbol{I} + 2\mu\boldsymbol{E} \tag{4.10}$$

$$\delta\boldsymbol{t} = \lambda(\boldsymbol{\nabla}\cdot\mathbf{s})\,\boldsymbol{I} + 2\mu\boldsymbol{e} \tag{4.11}$$

where $\boldsymbol{I}$ is the identity tensor, $\boldsymbol{E}$ and $\boldsymbol{e}$ are the linear strain tensors in $\mathfrak{S}$ and $\mathfrak{s}$, respectively, and λ and μ are the Lamé parameters.

To be complete, we must also append boundary and continuity conditions to the equations of motion. They are given on page 885 of Rogister and Rochester (2004, Section 2.3).

To take the electromagnetic field into account, we would have to add the Laplace-Lorentz force in Eqs (4.1) or (4.4), as well as Maxwell's equations.

4.5 Resolution methods

The most difficult step of the modelling of the Earth's nutation and polar motion - Step 3 on page 30 - is to solve the set of partial differential equations written in Section 4.4.

Since we only consider free or forced periodic oscillations, the displacement field, the variation of the gravity potential, the external force field and the variable angular velocity $\boldsymbol{\Omega}$ are proportional to $e^{i\omega t}$ or $e^{i\omega T}$. In Eqs (4.1) and Eqs (4.4), the time derivatives are therefore replaced by $i\omega$. To solve either Eqs (4.1)-(4.3) or (4.4)-(4.6), we decompose the displacement field into spheroidal and toroidal vectors [see Eq. (40) of Rogister and Rochester (2004, Section 2.3)]. We then develop the spheroidal and toroidal scalars, as well as the variation of the gravity potential, into series of spherical harmonics $Y_\ell^{\pm1}(\theta, \varphi)$:

$$\mathbf{S} = \sum_{\ell=1,3,5,\ldots}^{\infty} (\boldsymbol{\mathcal{T}}_\ell^{\pm1} + \boldsymbol{\Sigma}_{\ell+1}^{\pm1}) \tag{4.12}$$

$$\Phi' = \sum_{\ell=2,4,6,\ldots}^{\infty} \Phi_\ell'^{\pm1} Y_\ell^{\pm1}(\theta, \varphi) \tag{4.13}$$

$$\mathbf{s} = \sum_{\ell=1,3,5,\ldots}^{\infty} (\boldsymbol{\tau}_\ell^{\pm1} + \boldsymbol{\sigma}_{\ell+1}^{\pm1}) \tag{4.14}$$

$$\phi' = \sum_{\ell=2,4,6,\ldots}^{\infty} \phi_\ell'^{\pm1} Y_\ell^{\pm1}(\theta, \varphi) \tag{4.15}$$

where $\boldsymbol{\mathcal{T}}_\ell^m$ and $\boldsymbol{\tau}_\ell^m$ are toroidal displacements of degree ℓ and order ±1, and $\boldsymbol{\Sigma}_{\ell+1}^m$ and $\boldsymbol{\sigma}_{\ell+1}^m$ are spheroidal displacements of degree $\ell+1$ and order ±1. For the angular variables θ and φ, we will

take the physical colatitude and longitude, respectively, as in Smith (1974) or Sasao et al. (1980). The latter paper, inspired by Molodensky's work (1961), paved the way for further studies based on the angular momentum approach, such as those by Mathews et al. (1991, 2002), and ultimately the model IAU 2000. Other choices for θ and φ were made by Rogister and Rochester (2004, Section 2.3) for the LM approach and Rochester and Crossley (2008) for the AM approach. The coupling between spheroidal and toroidal displacements of different degrees is ruled by the departures from the spherical symmetry imposed by the apparent inertia forces and hydrostatic figure of the rotating Earth model.

For a given radius, the degree-1 and order ± 1 toroidal displacement is an infinitesimal rotation of the material particle about an equatorial axis. If, moreover, it is a linear function of radius, then the Earth rotates as if rigid about that equatorial axis, which is a nutational or a polar motion. The series with orders ± 1 starting at the degree-1 toroidal displacement therefore contain nutation and polar motion, which are the same motion viewed in different reference frames : nutation is the motion of a rotation axis with respect to the space-fixed Z axis of $\mathfrak{S}$, polar motion is the motion of the same rotation axis with respect to an Earth-fixed reference such as $\mathfrak{s}$. See Smith (1977), Moritz and Mueller(1987) or Dehant and Mathews (2007) for clear explanations on how polar motion and nutation are necessarily related. The series with order 0 starting at the degree-1 toroidal displacement contains the variations in the length of the day, which we do not consider here.

By projecting the unknowns $\mathbf{S}$, $\mathbf{s}$, Φ' and ϕ' on a vector spherical harmonics basis or a spherical harmonics basis, the partial differential equations that describe the infinitesimal Earth's motions are transformed in an infinite set of ordinary differential equations over radius. To compute analytical or numerical solutions, it is necessary to truncate the series. The IAU 1980 model rests on a development of $\mathbf{S}$ up to four terms (Wahr 1981 a, b) and makes no hypothesis on the radial dependence of the first toroidal term. Consistently, only two terms are retained in series (4.13) for the Eulerian variation of the gravity potential.

In the AM approach, the displacement and velocity fields depend on the choice of the reference frame $\mathfrak{s}$, which has not yet been defined. Because the Earth deforms, there is no such thing as an Earth-fixed rotating reference frame. Something approaching closely this concept can be constructed by minimizing in a least squares sense the deformation of the Earth. It turns out that the system of reference in which the total relative angular momentum of the Earth is zero has that property. It is called a Tisserand mean system and will be defined by Eqs (4.23) and (4.25). The relative displacement field is then assumed to be a deformational spheroidal displacement of degree 2 and order ± 1, the other terms being negligible. Actually, allowance must be made for the outer and inner cores to rotate relative to the mantle. Instead of choosing for $\mathfrak{s}$ a Tisserand mean system for the whole body, one therefore considers a Tisserand mean system for the mantle only. We can loosely say that it is mantle-fixed. To the accuracy implied by the truncature of series (4.14) after the degree-2 spheroidal term, Mathews et al. (1991) showed that other frames are equivalent to a Tisserand mean system for the mantle. In particular, a reference frame which has the same absolute angular velocity as the crust can be considered mantle-fixed. In the outer and inner cores, one then supposes that the displacement field takes the form of an infinitesimal rigid rotation, different in each layer, plus a degree-2 spheroidal term. Again, the separation of the displacement field into an infinitesimal rotation and a residual deformation is not unique and there is some arbitrariness in

the definition of the angular velocities $\mathbf{\Omega}_{\rm OC}$ and $\mathbf{\Omega}_{\rm IC}$ of the outer core and inner core, respectively. By choosing angular velocities in a such a way that the residual velocities contribute nothing to the total angular momenta of the outer and inner cores, one ascertains that the residual relative displacement is spheroidal of degree 2. Accordingly, only one term is retained in series (4.15) for the Eulerian variation of the gravity potential.

The truncatures and approximations described above are summarized by the following equations :

IAU 1980 - LM

Everywhere

$$\mathbf{S} \simeq \boldsymbol{\mathcal{T}}_1^{\pm 1} + \boldsymbol{\Sigma}_2^{\pm 1} + \boldsymbol{\mathcal{T}}_3^{\pm 1} + \boldsymbol{\Sigma}_4^{\pm 1} \qquad (4.16)$$

$$\Phi' \simeq \Phi_2'^{\pm 1} Y_2^{\pm 1} + \Phi_4'^{\pm 1} Y_4^{\pm 1} \qquad (4.17)$$

IAU 2000 - AM

– Mantle

$$\mathbf{s} \simeq \boldsymbol{\sigma}_2^{\pm 1} \qquad (4.18)$$

– Fluid outer core

$$\frac{d\mathbf{s}}{dt} \simeq \mathbf{\Omega}_{\rm OC} \times \mathbf{r} + \frac{d\boldsymbol{\sigma}_2^{\pm 1}}{dt} \qquad (4.19)$$

– Solid inner core

$$\frac{d\mathbf{s}}{dt} \simeq \mathbf{\Omega}_{\rm IC} \times \mathbf{r} + \frac{d\boldsymbol{\sigma}_2^{\pm 1}}{dt} \qquad (4.20)$$

Everywhere

$$\phi' \simeq \phi_2'^{\pm 1} Y_2^{\pm 1}(\theta, \varphi) \qquad (4.21)$$

In the LM approach, the finite set of ordinary differential equations obtained by replacing $\mathbf{S}$ and Φ in Eqs (4.1)-(4.3) by the truncatures (4.16) and (4.17) are then solved by numerical integration. This ends the description of the basic principles and some of the hypotheses and approximations at the root of the LM approach and IAU 1980 model of Earth's nutations. Other important approximations concern the accuracy to which the equilibrium shape of the rotating Earth model of reference must be taken into account in the equations of motion. Details can be found in Rogister and Rochester (2004, Section 2.3).

The ideas underlying the resolution of the equations (4.4)-(4.6) in the AM approach are (i) to parallel the analysis of the rotation of rigid bodies by establishing the conservation equations for the total absolute angular momentum of the Earth or part thereof to deal with the rotational part of the motion and (ii) to approximate the rotating reference Earth model by a spherical, non-rotating model to deal with the deformational part of the motion. The method has been described at length in numerous books (for instance, Moritz & Mueller 1987) and papers, so it does not need to be reproduced once more. I will only sketch an outline of the approach and get rid of the complications arising from the presence of the inner and outer cores by considering a one-layer Earth model. Because we are finished with the descritpion of the LM approach, the separation of the page into two columns is not useful anymore.

Denote the total absolute angular momentum of the Earth by $\mathbf{L}$:

$$\mathbf{L} = \int_V \rho \mathbf{r} \times (\boldsymbol{\Omega} \times \mathbf{r} + \frac{d\mathbf{s}}{dt})\, dV, \tag{4.22}$$

where V is the volume instantaneously occupied by the Earth. The inertia tensor being designated by $\boldsymbol{C}$, we have

$$\mathbf{L} = \boldsymbol{C} \cdot \boldsymbol{\Omega} + \mathbf{l}, \tag{4.23}$$

$\mathbf{l}$ being the relative angular momentum

$$\mathbf{l} = \int_V \rho \mathbf{r} \times \frac{d\mathbf{s}}{dt}\, dV. \tag{4.24}$$

Generally, $\boldsymbol{C}$ changes with time. We *define* $\boldsymbol{\Omega}$ in such a way that

$$\mathbf{l} = 0. \tag{4.25}$$

As already mentioned, the reference frame $\mathfrak{s}$ rotating with the absolute angular velocity $\boldsymbol{\Omega}(t)$ is called a Tisserand mean system.

An equation is now needed to determine $\boldsymbol{\Omega}(t)$. It is provided by the conservation equation for $\mathbf{L}$, named the Euler-Liouville equation [1]. In $\mathfrak{s}$, it writes

$$\frac{d\mathbf{L}}{dt} + \boldsymbol{\Omega} \times \mathbf{L} = \mathbf{M}, \tag{4.28}$$

where $\mathbf{M}$ is the moment of the external forces applied to the Earth. The departure from the steady rotation at constant angular velocity $\boldsymbol{\Omega}_0$ is small. So, if we put

$$\boldsymbol{\Omega} = \boldsymbol{\Omega}_0 + \boldsymbol{\omega}, \tag{4.29}$$

we have

$$|\omega| \ll |\Omega_0|. \tag{4.30}$$

1. It should be noted that the equations of conservation for the total linear momentum and total angular momentum are independent axioms in continuum mechanics. Their local forms are

$$\rho \frac{d\mathbf{v}}{dt} = \boldsymbol{\nabla} \cdot \boldsymbol{t} + \rho \mathbf{b} \tag{4.26}$$

and

$$\boldsymbol{t} = \tilde{\boldsymbol{t}}, \tag{4.27}$$

where $\mathbf{v}$ is the velocity, $\boldsymbol{t}$ is the Cauchy stress tensor, $\mathbf{f}$ is the body force per unit volume, which possibly includes the fictitious inertia forces, and $\tilde{\boldsymbol{t}}$ denotes the transpose of $\boldsymbol{t}$. Eq. (4.27), which means that the stress tensor is symmetric, holds when the particles have no intrinsic angular momentum and there are no body couples and couple stress. Truesdell and Toupin (1960, pp 538-546) name this case the *non-polar case*.

ω is not to be confused with the notation used elsewhere in this work for the frequency of an oscillation. Also, the components of the symmetric inertia tensor are

$$\boldsymbol{C} = \begin{pmatrix} A + c_{11} & c_{12} & c_{13} \\ c_{12} & A + c_{22} & c_{23} \\ c_{13} & c_{23} & C + c_{33} \end{pmatrix} \tag{4.31}$$

where the c_{ij}'s (i, $j = 1$, 2, 3) are the perturbations of the inertia tensor and are much smaller than the initial diagonal components A and C. By choosing the x_3-axis of the reference frame parallel to $\boldsymbol{\Omega}$, the three components of the conservation equation (4.28) are, to the first order in ω_i and c_{i3},

$$A\frac{d\omega_1}{dt} + (C - A)\omega_2\Omega_0 + \frac{dc_{13}}{dt}\Omega_0 - \Omega^2 c_{23} = M_1 \tag{4.32}$$

$$A\frac{d\omega_2}{dt} + (A - C)\omega_1\Omega_0 + \frac{dc_{23}}{dt}\Omega_0 + \Omega^2 c_{13} = M_2 \tag{4.33}$$

$$C\frac{d\omega_3}{dt} + \frac{dc_{33}}{dt}\Omega_0 = M_3. \tag{4.34}$$

To this order of approximation, the variations of the length of the day, contained in Eq. (4.34), decouple from the polar motion given by ω_1 and ω_2.

In Eqs (4.32)-(4.34), the c_{i3}'s are also unknowns. They, however, can be simply related to the degree-2 coefficients of the development of the gravitational potential in spherical harmonics :

$$\phi + \phi' = -\frac{GM_\oplus}{a}\left\{\frac{a}{r} - \sum_{\ell=1}^{\infty}\left(\frac{a}{r}\right)^{\ell+1}\left[J_\ell P_\ell(\cos\vartheta) + \sum_{m=1}^{\ell}\left(C_{\ell m}Y_{\ell m}^{c}(\vartheta,\varphi) + S_{\ell m}Y_{\ell m}^{s}(\vartheta,\varphi)\right)\right]\right\}, \tag{4.35}$$

where a and $M_\oplus$ are the equatorial semi-axis and mass of the Earth, respectively, and the spherical harmonics are defined by

$$Y_{\ell m}^{\left\{\begin{smallmatrix} c \\ s \end{smallmatrix}\right\}}(\vartheta,\varphi) = (-1)^m\sqrt{\frac{(2-\delta_{m0})(2\ell+1)(\ell-m)!}{4\pi(\ell+m)!}}P_{\ell m}(\cos\vartheta)\left\{\begin{matrix} \cos m\varphi \\ \sin m\varphi \end{matrix}\right\}, \tag{4.36}$$

where $P_{\ell m}(x)$ is the associated Legendre function. The relationship between the degree-2 coefficients and the components of the inertia tensor are

$$J_2 = \frac{C - A}{M_\oplus a^2} + \frac{c_{33} - \frac{c_{11}+c_{22}}{2}}{M_\oplus a^2} \tag{4.37}$$

$$C_{21} = -\sqrt{\frac{12\pi}{5}}\frac{c_{13}}{M_\oplus a^2} \tag{4.38}$$

$$S_{21} = -\sqrt{\frac{12\pi}{5}}\frac{c_{23}}{M_\oplus a^2} \tag{4.39}$$

$$C_{22} = \sqrt{\frac{12\pi}{5}}\frac{c_{22} - c_{11}}{2M_\oplus a^2} \tag{4.40}$$

$$S_{22} = -\sqrt{\frac{12\pi}{5}}\frac{c_{12}}{M_\oplus a^2}. \tag{4.41}$$

Although I use the same usual notations employed for the *static* Earth's gravitational potential, the coefficients J_ℓ, $C_{\ell m}$ and $S_{\ell m}$ are here functions of time. Initially, the gravitational potential was

$$\phi = -\frac{GM_\oplus}{a}\left[\frac{a}{r} - \frac{C-A}{M_\oplus a^2}\frac{a^3}{r^3}P_2(\cos\vartheta)\right]. \tag{4.42}$$

One sees that the c_{i3} are proportional to the degree-2 harmonic components of ϕ', which is a solution of Poisson's equation (4.6). The goal of the AM approach is to avoid the direct resolution of Eqs (4.4)-(4.6), which is made in the LM approach. To simplify, the variation of the gravitational potential ϕ' of the rotating model is approximated by the variation of the gravitational potential of the corresponding spherical non rotating model caused by the variation of the centripetal force $\rho[\mathbf{\Omega}\times(\mathbf{\Omega}\times\mathbf{r}) - \mathbf{\Omega}_0\times(\mathbf{\Omega}_0\times\mathbf{r})]$, together with the external tidal force. To the first order in ω_1 and ω_2, the variation of the centrifugal force is -ρ times the gradient of

$$\phi_{\rm cent} = \Omega_0(\omega_1 x_1 x_3 + \omega_2 x_2 x_3) \tag{4.43}$$

$$= -\sqrt{\frac{4\pi}{15}}\Omega_0 r^2\left[\omega_1 Y_{21}^c(\vartheta,\varphi) + \omega_2 Y_{21}^s(\vartheta,\varphi)\right]. \tag{4.44}$$

The deformation due to the variation of the centripetal force is called the pole tide. Because the equations of motion have been linearized, ϕ' is proportional to the exciting potential $\phi_{\rm ext}$, which here includes both the tidal potential and $\phi_{\rm cent}$. Their ratio only depends on the structure of the Earth model and frequency of the motion. When dealing with a spherical non rotating Earth model and spherical harmonics expansions, the Love and Shida numbers are non-dimensional numbers commonly used to represent the ratios between the displacement or variation of the gravitational potential and the exciting potential of the same degree. For ϕ', the degree-ℓ Love number k_ℓ is defined by

$$\phi'_{\ell m}\left\{\begin{matrix} c \\ s \end{matrix}\right\} = k_\ell \phi_{{\rm ext}\,\ell m}\left\{\begin{matrix} c \\ s \end{matrix}\right\}, \tag{4.45}$$

the potential being computed at the surface $r = R$. It is independent of m because the Earth model is non rotating and spherical. Consequently,

$$c_{13} = \sqrt{\frac{5}{12\pi}}\frac{R^3}{G}k_2\phi_{\rm ext}{}^c_{21}(R) \tag{4.46}$$

$$c_{23} = \sqrt{\frac{5}{12\pi}}\frac{R^3}{G}k_2\phi_{\rm ext}{}^s_{21}(R) \tag{4.47}$$

and the only unknowns subsisting in Eqs (4.32) and (4.33) are ω_1 and ω_2.

The rotation of the outer (Sasao et al. 1980) and inner (Mathews et al. 1991) cores, described by $\mathbf{\Omega}_{\rm OC}$ and $\mathbf{\Omega}_{\rm IC}$, can be similarly incorporated in the modeling by considering the equations of conservation of the angular momentum of the two layers.

To close this chapter, we summarize the comparison between the AM and LM approaches in the next section.

4.6 Conclusions

The IAU 1980 nutation-precession model was based on the linear momentum (LM) approach that consists in solving the equations of motion (4.1)-(4.3) in a system of reference $\mathfrak{S}$ steadily rotating about a fixed axis. For the sake of numerical computation, the displacement field and gravitational potential variation were approximated by the forms (4.16) and (4.17).

The IAU 2000 nutation-precession model is based on the angular momentum (AM) approach that consists in solving (4.28) in a system of reference rotating with the mantle at a variable angular velocity, together with the equations of motion of a non-rotating spherical model deformed by the variable centripetal force.

Let us make the comparison easier by describing the mantle displacement in $\mathfrak{S}$ for the two approaches. For the LM approach, it is approximated by (4.16), without any assumptions on the different terms. For the AM approach, it would be a supposedly rigid nutation at angular velocity $\boldsymbol{\omega}$ plus a deformation that is assumed to be almost the same as the deformation of the corresponding non-rotating spherical Earth model. A similar comparison can be made for the displacements in the inner and outer cores. As such, the AM approach allows for neither the computation of the seismic normal modes of the rotating Earth model nor the study of the core spectrum, which is strongly influenced by rotation.

Chapitre 5

Avoided crossings

> Eigenproblems can be nasty. [...] Nevertheless, [...], even nasty eigenproblems can be solved with high accuracy.
>
> Boyd (2001)

5.1 Introduction

In Rogister and Valette (2005, 2009, Sections 3.2.2 and 3.2.3), we have seen that the outer core structure, quantified by the squared Brunt-Väisälä frequency N^2, influences the frequencies of the rotational modes and core pseudo-modes. To simplify, we have assumed that N^2 is constant throughout the outer core, so we had to deal with a single parameter only. For specific values of N^2, the frequencies of a given rotational mode, for instance the Chandler wobble, and a core pseudo-mode closely approach but are not equal. The plot of the two eigenfrequencies versus N^2 show that the curves do not intersect : they avoid crossing.

Avoided crossings of frequencies of oscillatory motions are ubiquitous in many fields of physics and geophysics. In the simplest cases, they occur when there are two degrees of freedom, allowing for the existence of two normal modes at most, and a single parameter is varied. In the following, we shall consider various examples to illustrate the phenomenon. We will start with the oscillations of two coupled LC electrical circuits [1], carry on with the energy levels of an electron in diatomic molecules, and the coupling of surface gravity waves in an ocean and finish with the reversals of the Earth's magnetic field.

5.2 LC circuits coupling

We first consider an electrical LC circuit, made up of a capacitor and a coil. The capacities of the capacitor will be denoted by C and the inductance of the coil, L. If the capacity is initially charged with a charge q_0, the charge on the capacitor q and current intensity $i = -dq/dt$ in the

1. The small oscillations of a double pendulum are a formally equivalent example.

circuit at a later time t are related by

$$\frac{q}{C} - L\frac{di}{dt} = 0. \tag{5.1}$$

The solution for both the charge and current is an oscillation with eigenfrequency

$$\omega = \frac{1}{\sqrt{LC}}. \tag{5.2}$$

We next consider two electrical circuits each made up of a capacitor and a coil. The capacities of the capacitors will be denoted by C_1 and C_2 and the inductances of the coils, L_1 and L_2. The coils are sufficiently close to each other for their mutual inductance to be taken into account (Fig. 5.1). Let q_1 and $i_1 = -dq_1/dt$ be the charge on the first capacitor and current intensity in the first

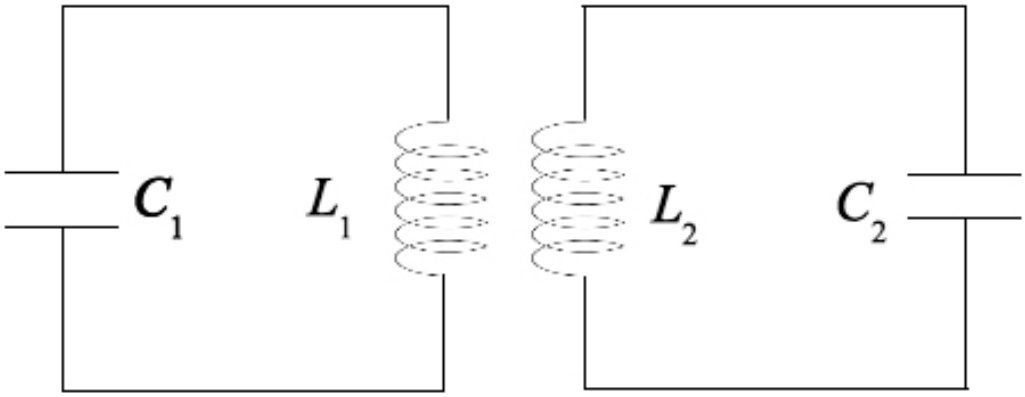

FIGURE 5.1 – Coupled LC electrical circuits

circuit, respectively. Similarly, q_2 and i_2 are defined for the second circuit. The mutual inductance will be denoted by M. Because of the coupling between the coils, the charges and current intensities obey the following coupled differential equations :

$$\frac{q_1}{C_1} - L_1\frac{di_1}{dt} - M\frac{di_2}{dt} = 0 \tag{5.3}$$

$$\frac{q_2}{C_2} - L_2\frac{di_2}{dt} - M\frac{di_1}{dt} = 0. \tag{5.4}$$

We try a solution of the form

$$q_1 = q_1^0 e^{i\omega t} \tag{5.5}$$

$$q_2 = q_2^0 e^{i\omega t} \tag{5.6}$$

and obtain the two eigenfrequencies

$$\omega_\pm^2 = \frac{\omega_1^2 + \omega_2^2 \pm \sqrt{(\omega_1^2 + \omega_2^2)^2 - 4(1 - \alpha_1\alpha_2)\omega_1^2\omega_2^2}}{2(1 - \alpha_1\alpha_2)} \tag{5.7}$$

where

$$\omega_1 = \frac{1}{\sqrt{L_1 C_1}} \tag{5.8}$$

$$\omega_2 = \frac{1}{\sqrt{L_2 C_2}} \tag{5.9}$$

$$\alpha_1 = \frac{M}{L_1} \tag{5.10}$$

$$\alpha_2 = \frac{M}{L_2}. \tag{5.11}$$

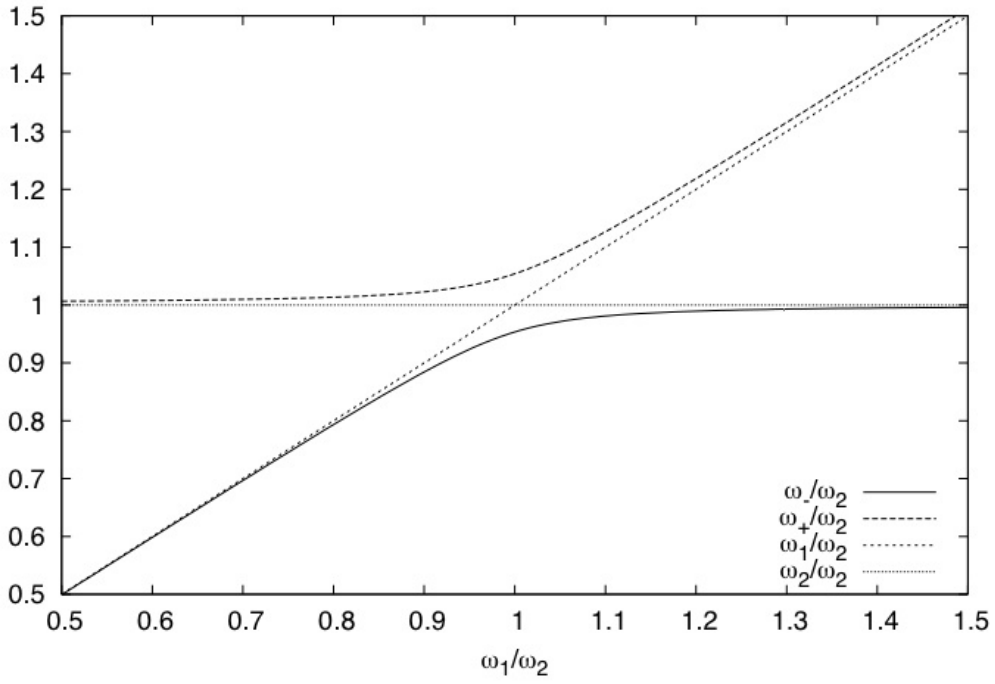

FIGURE 5.2 – Eigenfrequencies of LC circuits, scaled to ω_2, as a function of ω_2/ω_1. ω_1 and ω_2, given by Eq. (5.2), are the eigenfrequencies of two uncoupled LC circuits. ω_- and ω_+, given by Eq. (5.7), are the eigenfrequencies of two coupled LC circuits. In the last formula, we have chosen $\alpha_1 = \alpha_2 = 0.1$.

Fig. 5.2 shows plots of ω_1/ω_2, ω_2/ω_2, ω_-/ω_2, and ω_+/ω_2 as a function of ω_1/ω_2. For an illustrative purpose, we have chosen $\alpha_1 = \alpha_2 = 0.1$, which is kept fixed. This implies that $L_1 = L_2$ and the self inductances are ten times bigger than the mutual inductance. One can therefore expect a weak coupling between the two circuits, which is confirmed by the Figure. In this case, varying the ratio ω_1/ω_2 actually means that the ratio C_2/C_1 is varied. When either $\omega_1 \ll \omega_2$ or $\omega_1 \gg \omega_2$, the two eigenfrequencies ω_+ and ω_- are close to the eigenfrequencies ω_1 and ω_2 of the two uncoupled

circuits. When $\omega_1 \simeq \omega_2$, the two eigenfrequencies ω_+ and ω_- do not become equal but remain separated : the curves avoid crossing.

Fig. 5.2 must be compared to Fig. 5 of Rogister and Valette (2009, Section 3.2.3). Far from the avoided crossing, the Chandler wobble frequency behaves like ω_2 and the pseudo-core mode frequency behaves like ω_1. By analogy, the first and second LC circuits would play the role of points in the outer core and mantle, respectively.

To investigate the symmetry properties of the eigenfunctions, let us denote the eigenvectors associated to ω_+ and ω_- by, respectively,

$$\begin{pmatrix} q_1 \\ q_2 \end{pmatrix}_+ = \begin{pmatrix} A_1 \\ A_2 \end{pmatrix} e^{i\omega_+ t} \tag{5.12}$$

and

$$\begin{pmatrix} q_1 \\ q_2 \end{pmatrix}_- = \begin{pmatrix} B_1 \\ B_2 \end{pmatrix} e^{i\omega_- t}, \tag{5.13}$$

where A_1, A_2, B_1 and B_2 are constant. Using Eqs (5.3) and (5.4), we have

$$A_2 = \frac{\omega_1^2 - \omega_+^2}{\alpha_1 \omega_+^2} A_1 \tag{5.14}$$

and

$$B_2 = \frac{\omega_1^2 - \omega_-^2}{\alpha_1 \omega_-^2} B_1. \tag{5.15}$$

To simplify, let us assume that $\omega_1 = \omega_2 = \omega$ and $\alpha_1 = \alpha_2 = \alpha$. This is true if and only if $L_1 = L_2$ and $C_1 = C_2$. In that specific case [2], the two eigenfrequencies, which are at the avoided crossing on Fig. 5.2, are given by

$$\omega_\pm = \frac{\omega}{\sqrt{1 \mp \alpha}}. \tag{5.16}$$

Moreover, the amplitudes of the oscillations are related by

$$A_2 = -A_1 \tag{5.17}$$

and

$$B_2 = B_1. \tag{5.18}$$

The two circuits oscillate in opposition of phase at the eigenfrequency ω_+ but oscillate in phase at the eigenfrequency ω_-. Again, this is to be compared with Fig. 7 of Rogister and Valette (2009,

2. The analogous specific case for the double pendulum occurs when the two masses and the lengths R of the pendulums are the same. However, the amplitudes of the oscillations of the masses, at either one or the other eigenfrequency, are not the same. Indeed, one has $A_2 = -\sqrt{2}A_1$ and $B_2 = \sqrt{2}B_1$, where A_1 and B_1 (resp. A_2 and B_2) are the amplitudes of the oscillations of the higher (resp. lower) mass at the two eigenfrequencies $\omega_\pm^2 = g(2 \pm \sqrt{2})/R$. This is due to the fact that the double pendulum is not symmetrical with respect to the two masses, whereas the system made up of two identical LC circuits is symmetrical.

Section 3.2.3), which shows the eigenfunctions of two Earth normal modes at an avoided crossing. The eigenfunctions of these two modes contain both a wobble of the mantle and oscillations in the outer core. Let us consider a given point in the mantle and a given point in the outer core. The amplitude of the displacement of the mantle point is the same in the two modes (the amplitude of a normal mode actually depends on the excitation source ; in Rogister and Valette's numerical computation, no excitation source is considered and the amplitude of the modes is arbitrarily set in such a way that $W_1^{-1} = 1$ m at the surface). In our analogy, this translates into $A_2 = B_2$. Comparing the oscillations in the outer core, we see that approximately $A_1 \simeq -B_1$. If the two points that we picked in the mantle and outer core oscillate with equal amplitudes, we recover, at least approximately, Eqs (5.17) and (5.18).

5.3 Diatomic molecules

Let us consider, for instance, the ion H_2^+, where a single electron is orbiting two fixed protons. This is a particular case of the three-body problem in quantum mechanics. The energy levels E of the electron are the eigenvalues of the time-independent Schrödinger equation

$$\hat{H}\psi = E\psi, \tag{5.19}$$

$\hat{H}$ being the Hamiltonian and ψ, the electron wave function. The Hamiltonian is

$$\hat{H} = -\frac{\hbar^2}{2m_e}\nabla^2 - \frac{e^2}{4\pi\epsilon_0}\left(\frac{1}{r_1} + \frac{1}{r_2}\right), \tag{5.20}$$

where m_e and e are the mass and electrical charge of the electron, respectively, ∇^2 is the Laplacian, $\hbar$ is Planck's constant divided by 2π, and r_1 and r_2 are the distances from the protons to the electron. Eq. (5.19) is separable in the prolate spheroidal coordinates ξ, λ, ϕ defined by

$$\xi = \frac{r_1 + r_2}{R} \tag{5.21}$$

$$\lambda = \frac{r_1 - r_2}{R} \tag{5.22}$$

and ϕ is the rotation angle about the axis passing through the two protons. R is the distance between the protons. ξ, λ, ϕ can take on the following values : $\xi \geq 1$, $-1 \leq \lambda \leq 1$ a and $0 < \phi < 2\pi$. The solution ψ can indeed be written

$$\psi = \Xi(\xi)\Lambda(\lambda)e^{im\phi}, \tag{5.23}$$

where m is an integer, and Ξ and Λ are solutions of the ordinary differential equations

$$\frac{d}{d\xi}\left[(\xi^2 - 1)\frac{d\Xi}{d\xi}\right] + \left[A + \frac{m_e R^2 E}{2\hbar^2}\xi^2 + \frac{m_e e^2 R}{8\pi\hbar^2\epsilon_0}\xi - \frac{m^2}{\xi^2 - 1}\right]\Xi = 0 \tag{5.24}$$

$$\frac{d}{d\lambda}\left[(1 - \lambda^2)\frac{d\Lambda}{d\lambda}\right] + \left[-A - \frac{m_e R^2 E}{2\hbar^2}\lambda^2 - \frac{m^2}{1 - \lambda^2}\right]\Lambda = 0, \tag{5.25}$$

A being a separation constant. By imposing appropriate boundary conditions to the ODEs, two extra quantum numbers will characterize the eigenvalues E. No comprehensive analytical solution is presently known, contrary to what Linus Pauling expected in 1928 [3]. However, asymptotic expansions in R^{-1} have been derived (Čížek et al. 1986). When $R \to \infty$, the eigenvalues tend to the eigenvalues of the hydrogen atom. Moreover, for $m = 0$, implicit solutions for the eigenvalues and a description of their structure have been obtained by Scott et al. (2006) using computer algebra.

Nevertheless, von Neumann and Wigner (1929) have established that, in diatomic molecules, the energy levels of electronic states of the same symmetry may avoid crossing when the internuclear distance R is varied. The application of this non-crossing rule, which is based on a first-order perturbation theory, actually depends on the accurate definition of the symmetry properties of the system (Hatton 1976), and sometimes provides incorrect predictions. Numerical solutions of the exact equations have shown that avoided crossings actually occur. Fig. 5.3 (taken from Hatton 1986) is an illustration of the numerically computed energy states of the electron of the ion BH^{5+} as a function of the internuclear distance, with an avoided crossing between two energy states.

Avoided crossings are extensively studied in quantum chemistry. Since the first calculation by von Neumann and Wigner (1929), avoided crossings have been put in a more general frame where many complex parameters are varied and the eigenvalues are complex, giving rise to the concept of exceptional points that are the points in the complex parameter plane where two eigenvalues coalesce (see Heiss (2000) for a generic example of a two-dimensional problem).

5.4 Stability of water waves

Infinitesimal surface gravity waves can propagate on an ocean of infinite horizontal extent and constant depth H. Assuming that they travel in the x-direction, the displacement of the surface is given by

$$\zeta_0(x,t) = a\cos(kx - \sigma_0 t), \tag{5.26}$$

where a is the amplitude of the wave, the pulsation σ_0 and wave number k obey, to a first-order approximation, the dispersion relation

$$\sigma_0^2 = gk\tanh kH \tag{5.27}$$

Under the surface, the amplitude of the oscillation decreases exponentially as a function of depth. When the wavelength is much smaller than the ocean depth, one has

$$\lim_{kH\to\infty} \sigma_0^2 = gk. \tag{5.28}$$

Still in the approximation of infinite depth, Stokes (1847) took into account the finite amplitude of the wave and obtained from a third-order approximation

$$\zeta_2(x,t) = a\cos(kx - \sigma_2 t) - \frac{1}{2}ka^2\cos 2(k - \sigma_2 t) + \frac{3}{8}k^2a^3\cos 3(k - \sigma_2 t) \tag{5.29}$$

3. "Many efforts have been made to solve these equations analytically, but so far they have all been unsuccessful, and little has been published regarding them. [...] It is probable, in view of the vigor with which it is being attacked, that the problem will be solved completely before very long." (Pauling 1928).

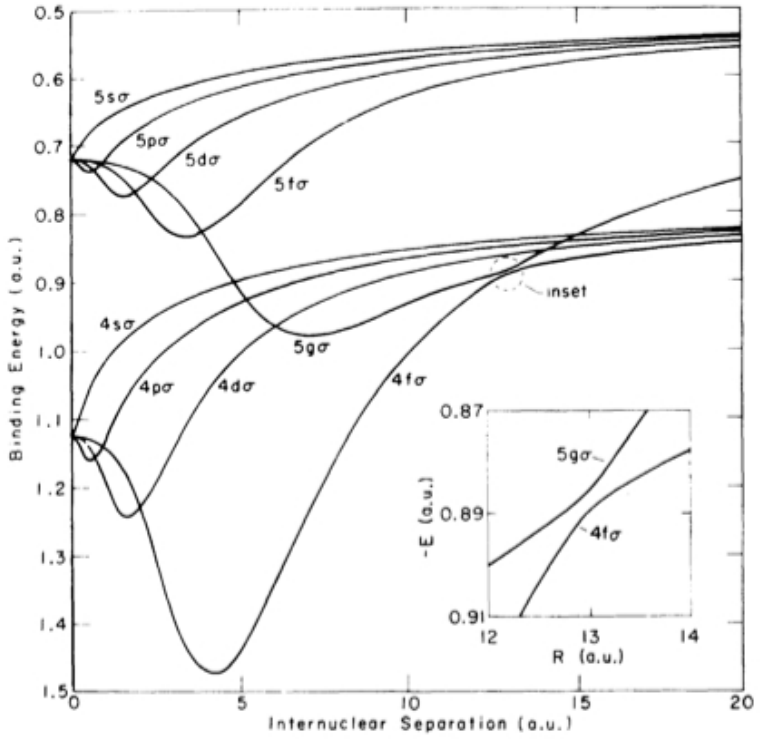

FIGURE 5.3 – Energy states of the electron of the ion BH^{5+} as a function of the internuclear distance. An avoided crossing is enlarged in the bottom right frame. Not all the crossings are avoided. Taken from Hatton (1976).

and

$$\sigma_2^2 = gk\left(1 + \frac{a^2}{k^2}\right). \tag{5.30}$$

The frequency of the motion now depends on the amplitude of the wave.

To study the stability of the surface gravity waves, McLean (1982) considered infinitesimal oscillatory disturbances to the Stokes wave of wavenumber k. The perturbation $\zeta'(x, y, t)$ to the surface displacement $\zeta_2(x, t)$ is searched under the form

$$\zeta'(x, y, t) = e^{-i\sigma t} e^{i(pkx+qky)} \sum_{j=-\infty}^{\infty} a_m e^{ijkx}, \tag{5.31}$$

where p and q are real numbers. σ is then a solution of an eigenvalue problem that provides eigenfrequencies σ_m, with m an integer. When $\zeta_2(x, t) = 0$, the eigenfrequencies in a reference frame comoving with the unperturbed Stokes wave are given by

$$\sigma_m = -(p + m)\sqrt{gk} + s\sqrt{gk\sqrt{(p + m)^2 + q^2}}, \tag{5.32}$$

where $s = \pm 1$ is called the signature. Since they are real, the oscillations are stable.

When the wave steepness ka is different from zero, the eigenfrequencies are no longer given by (5.32) but they depend on ka. As ka is increased, two real eigenfrequencies can approach each other and two phenomena can be observed : either they remain real and avoid crossing, or they collide to yield a single complex eigenfrequency, which results in an unstable oscillation. The second case, coined 'bubble of instability', is shown in Fig. 5.4 (taken ftom Mac Kay and Saffman 1986).

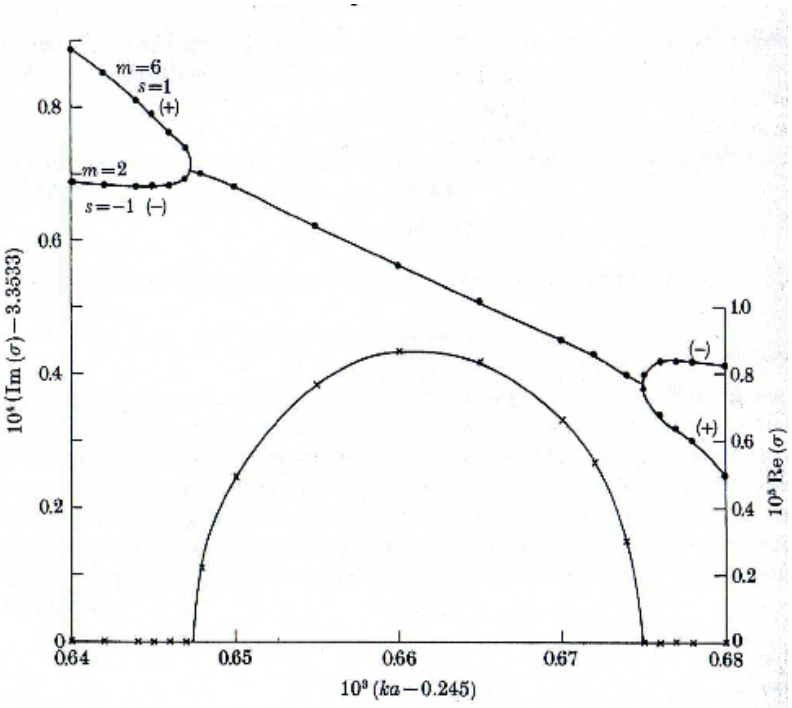

FIGURE 5.4 – Bubble of instability for surface gravity waves. The real and imaginary parts of eigenfrequencies of the small pertubations to a Stokes wave are plotted as a function of the wave steepness ka. As ka increases, the eigenfrequencies, which are first both real, collide to yield a single complex eigenfrequency, then separate to provide two real eigenfrequencies back. Taken from MacKay and Saffman (1986).

Fig. 13 in Rogister and Valette (2009, Section 3.2.3), which shows both the FCN frequency and a pseudo-core mode frequency as a function of the constant squared Brunt-Väisälä in the outer core, is probably a bubble of instability. Confirmation should be brought by extending our numerical code to compute the complex eigenfrequencies of the Earth normal modes.

Instability of surface gravity waves is one of the few mechanisms that could explain the generation of rogue waves, which are giant waves that abruptly appear at the surface of the ocean (Kharif et al. 2009).

5.5 Geodynamo

The concepts of bubble of instability and exceptional points are certainly appealing to the geodynamo theoretists, who have to explain complex changes in the dynamo regime, including the steady behavior of the Earth's magnetic field interrupted by irregular reversals of its main, dipolar, component.

So, Gubbins and Gibbons (2002) considered a kinematic dynamo, which is a dynamo in which the flow field $\mathbf{V}$ is prescribed and $\mathbf{B}$ is obtained by solving Maxwell's equations (Section 2.4.1). Expanded into vector spherical harmonics in a spherical configuration, their velocity field had the form

$$\mathbf{V} = \mathbf{T}_1^0 + \mathbf{S}_2^0 + \mathbf{S}_2^{-2} + \mathbf{S}_2^2, \tag{5.33}$$

where $\mathbf{T}$ and $\mathbf{S}$ denote toroidal and spheroidal fields, respectively, and the subscripts (resp. superscripts) are the harmonic degrees (resp. orders). The first term is a, possibly differential, rotation about the z-axis, the second term is the meridional circulation and the last two terms represent convection rolls. Gubbins and Gibbons (2002) defined two parameters D and M that are the relative kinetic energy contained in the rotational and meridional flows, respectively. Also defining the magnetic Reynolds number by

$$R_m = UL\sigma\mu_0 \tag{5.34}$$

where U and L are typical velocity and length scales of the flow, and reminding us that $\mathbf{B}$ is divergence free, the induction equation (2.9) becomes

$$\frac{\partial \mathbf{B}}{\partial t} = R_m \boldsymbol{\nabla} \times (\mathbf{V} \times \mathbf{B}) - \nabla^2 \mathbf{B}, \tag{5.35}$$

where all the variables have been adimensionalized. Searching for a dipolar magnetic induction of the form

$$\mathbf{B}_d = \hat{\mathbf{B}}_d e^{i\omega t} \tag{5.36}$$

led to an eigenvalue problem. If the growth rate $-\Im(\omega)$ is positive, the field is growing, which is a condition for the dynamo to function. The magnetic field is steady if both $\Im(\omega)$ and $\Re(\omega)$ are zero. Fig. 5.5 shows $-\Im(\omega)$ as a function of R_m for a fixed D and a varying M. Following the curves from the left to the right in, for instance, the top left frame, two purely imaginary eigenvalues (i.e. $\Re(\omega) = 0$) that give a growing or decaying field according to their sign join to give a single complex eigenvalue corresponding to an oscillatory magnetic induction. At $R_m \simeq 1300$, the complex eigenvalue splits into two purely imaginary eigenvalues, which give two exponentially growing solutions. The existence of dynamo solutions therefore depends on a fine tuning of the three parameters M, D and R_m.

A tentative explanation for the reversal of the Earth's magnetic field as a consequence of the occurrence of exceptional points in the spectrum of the magnetic oscillations was given by, for instance, Stefani and Gerbeth (2005) who considered an α^2 turbulent dynamo model in a sphere.

For that model, $\mathbf{B}$ is split into a mean field $\overline{\mathbf{B}}$ and a small turbulent field $\mathbf{b}'$. The mean field $\overline{\mathbf{B}}$ is then a solution of

$$\frac{\partial \overline{\mathbf{B}}}{\partial t} = \boldsymbol{\nabla} \times \alpha \overline{\mathbf{B}} - \nabla^2 \overline{\mathbf{B}}, \tag{5.37}$$

where α is a turbulent parameter, which is assumed to depend on the radius r and time t. By searching for dipolar solutions of this equation and plotting the growth rate of $\overline{\mathbf{B}}$ as a function of the constant term C of the radial expansion of α, Stefani and Gerbeth (2005) found exceptional points where two eigenvalues coalesce. The exceptional points mark the transition from an oscillatory regime to a non-oscillatory regime, and vice versa. Fo a given C, since α is a function of time, the exceptional points and the growth rates change, allowing for regime transitions and reversal of the dipolar field.

5.6 Conclusions

The goal of this chapter was to exemplify the concept of avoided crossing of eigenfrequencies when a parameter of a physical system is varied. In doing so, we encountered another kind of eigenfrequencies coupling that possibly leads to instabilities.

Two coupled LC circruits, wich is a simple oscillating physical system with two degrees of freedom, has first been considered. Analytical solutions for the two eigenfrequencies show that, when plotted as a function of a parameter of the system, their curves avoid crossing. Far from the crossing, the eigenfrequencies tend to the eigenfrequencies of two uncoupled LC circuits.

Second, an apparently simple example from quantum mechanics, the H_2^+ ion, has been briefly touched upon. In the absence of analytical solution for the energy states of the electron, wich are the eigenvalues of the Hamiltonian, one must resort to numerical approaches to show avoided crossings. Theoretical considerations also show that they actually occur.

Third, a second kind of interaction between eigenfrequencies has been described by considering the stability of finite surface gravity waves in an ocean of infinite horizontal extent. Indeed, the oscillatory disturbances to the basic finite-amplitude water waves are obtained by solving an eigenvalue problem. When the wave steepness changes, the real eigenfrequencies of two perturbations can either avoid crossing or merge into a single complex eigenfrequency associated to an instability of the basic gravity wave.

We took the fourth and final example from kinematic and turbulent dynamo theories for the Earth's magnetic field. There, the growth rate and oscillatory regime of the magnetic field depend on physical parameters such as the core viscosity or the flow and turbulence in the core. If those parameters change with time, the dynamo can shift from an oscillatory to a non-oscillatory regime, and inversely. This mechanism could explain the reversals of the dipolar magnetic field.

Still other complex occurrences of avoided crossings that involve gravity, sound and magnetic waves can be found in astrophysics (see, for instance, Hasan and Christensen-Dalsgaard 1992).

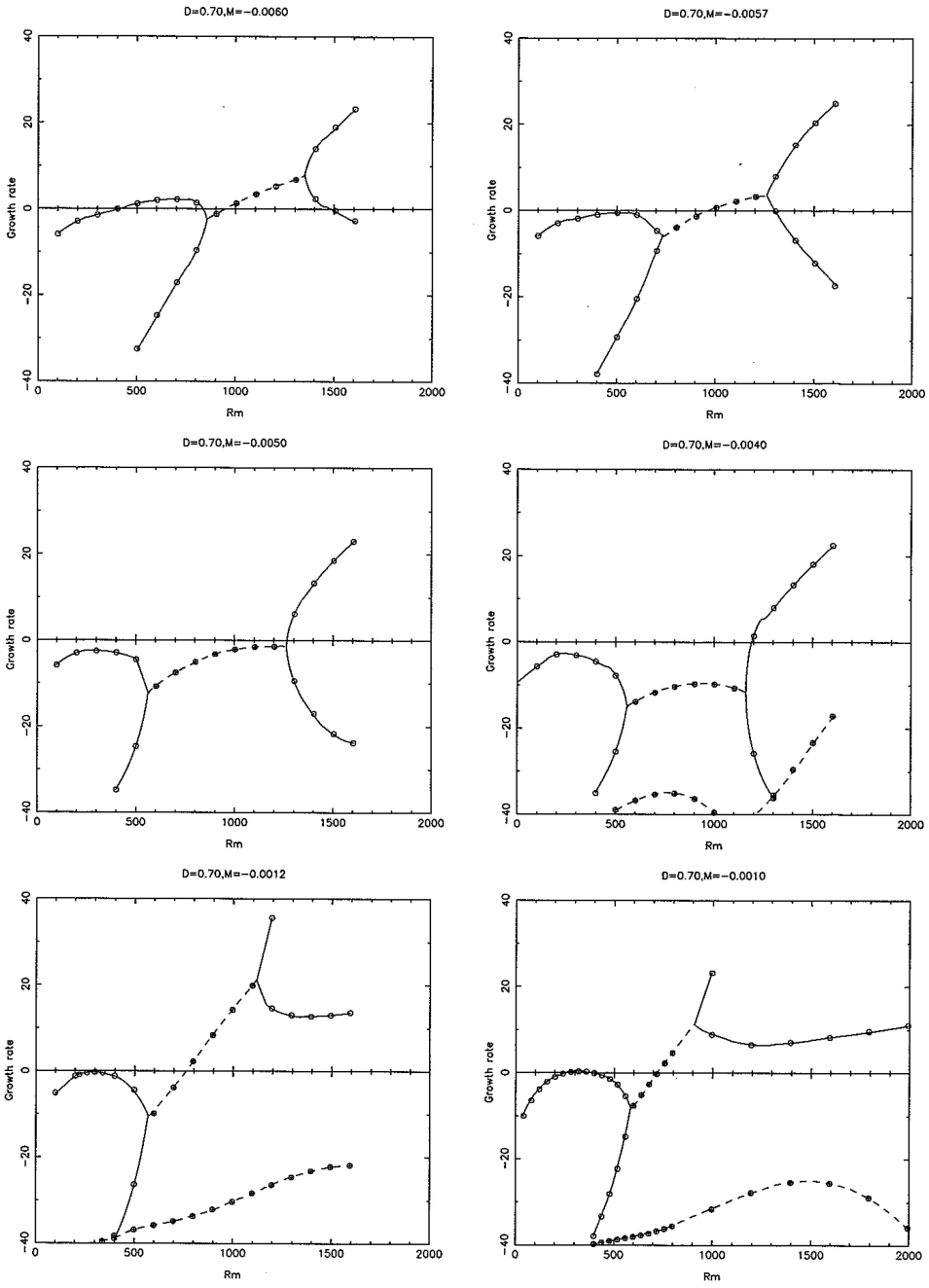

FIGURE 5.5 – Growth rate (= - $\Im(\omega)$) of dipolar magnetic modes as a function of the magnetic Reynolds number R_m, for a fixed $D = 0.7$ and M varying from -0.006 to -0.001. The empty circles represent purely imaginary eigenvalues ω, filled circles represent complex eigenvalues (whose real part is not shown here). Taken from Gubbins and Gibbons (2002).

Bibliographie

[1] Boyd JP : Chebyshev and Fourier spectral methods, 2nd ed., Mineola, New York : Dover, 2001.

[2] Buffett BA : Constraints on magnetic energy and mantle conductivity from the forced nutations of the Earth. J Geophys Res 97 B13 : 19581–19597, 1992.

[3] Buffett BA, Mathews PM, Herring TA : Modeling of nutation and precession : Effects of electromagnetic coupling. J Geophys Res 107 B4 : 2070, doi :10.1029/2000JB000056, 2002.

[4] Čížek J, Damburg RJ, Graffi S, Grecchi V, Harrell II EM, Harris JG, Nakai S, Paldus J, Propin RKh, Silverstone HJ : 1/R expansion for $H2^+$: Calculation of exponentially small terms and asymptotics. Phys Rev 33(1) : 12–54, 1986.

[5] Crossley DJ, Smylie DE : Electromagnetic and viscous damping of core oscillations. Geophys J R astr Soc 42 : 1011–1033, 1975.

[6] Dehant V, Mathews PM : Earth rotation variations. In *Treatise on Geophysics*, ed. Herring TA, vol. 3 Geodesy, Amsterdam, Pays-Bas : Elsevier, 295–349, 2007.

[7] Ghil M, Allen MR, Dettinger MD, Ide K, Kondrashov D, Mann ME, Robertson AW, Saunders A, Tian Y, Varadi F, Yiou P : Advanced spectral methods for climatic time series. Rev Geophys 40 : 1–41, doi :10.1029/2001RG000092, 2002.

[8] Gubbins D, Gibbons S : Three-dimensional dynamo waves in a sphere. Geophys Astrophys Fluid Dyn 96 : 481–498, doi :10.1080/0309192021000037003, 2002.

[9] Hasan SS, Chistensen-Dalsgaard : The influence of a vertical magnetic field on oscillations in an isothermal stratified atmosphere, Astophys J 396 : 311– 332, 1992.

[10] Hatton GJ : The noncrossing rule and spurious avoided crossings. Phys Rev A 14 (3) : 901–909, 1976.

[11] Heiss WD : Repulsion of resonance states and exceptional points. Phys Rev E 61 (1) : 929–932, 2000.

[12] Huang CL, Dehant V, Liao XH, Van Hoolst T, Rochester MG : On the coupling between magnetic field and nutation in a numerical integration approach. J Geophys Res 116, B03403, doi :10.1029/2010JB007713, 2011.

[13] Ivers DJ, Phillips CG : Scalar and vector harmonic spectral equations of rotating magnetohydrodynamics. Geophs J Int 175 : 955–974, doi :10.1111/j.1365-246X.2008.03944.x, 2008

[14] Kharif C, Pelinovsky E, Slunyaev A : Rogue waves in the ocean, Berlin Heidelberg : Springer, 2009.

[15] Landau LD, Lifshitz EM : Quantum Mechanics, Oxford : Pergamon Press, 3rd ed, 1977.

[16] MacKay RS, Saffman : Stability of water waves. Proc Roy Soc Lond A 406 : 115–125, 1986.

[17] Mathews PM, Buffett BA, Herring TA, Shapiro II : Forced nutations of the Earth : Influence of inner core dynamics. 1. Theory. J Geophys Res 96 B5 : 8219–8242, 1991.

[18] Mathews PM, Herring TA, Buffett BA : Modeling of nutation and precession : New nutation series for nonrigid Earth and insights into the Earth's interior. J Geophys Res 107 B4 : 2068. doi :10.1029/2001JB000390, 2002.

[19] McLean JW : Instabilities of finite amplitude water waves. J Fluid Mech 114 : 315–330, 1982.

[20] Molodensky MS : The theory of nutation and diurnal Earth tides. Comm Obs R Belgique 58 : 25–56, 1961.

[21] Moritz H, Mueller II : Earth rotation : Theory and observation, New York : Ungar, 1987.

[22] Pauling L : The application of the quantum mechanics to the structure of the hydrogen molecule and hydrogen molecule-ion and to related problems. Chem Rev 5 (2) : 173–213, 1928.

[23] Ritzwoller M, Masters G, Gilbert F : Observations of anomalous splitting and their interpretation in terms of aspherical structure. J Geophys Res 91 : 10203–10228, 1986.

[24] Rochester MG, Crossley DJ : Earth's long-period wobbles : a Lagrangean description of the Liouville equations. Geophys J Int 176 : 40–62, doi :10.1111/j.1365-246X.2008.03991.x, 2008.

[25] Rogister Y : On the diurnal and nearly diurnal free modes of the Earth. Geophys J Int 144 : 459–470, 2001. (Section 2.2).

[26] Rogister Y : Splitting of seismic free oscillations and of the Slichter triplet using the normal mode theory of a rotating, ellipsoidal Earth. Phys Earth planet Inter 140 : 169–182, 2003. (Section 3.1.4)

[27] Rogister Y : Multiple inner core wobbles in a simple Earth model with inviscid core. Phys Earth planet Inter 178 : 8–15, doi :10.1016/j.pepi.2009.08.012, 2010. (Section 3.2.4)

[28] Rogister Y, Rochester MG : Normal-mode theory of a rotating Earth model using a Lagrangian perturbation of a spherical model of reference. Geoph J Int 159 : 874–908, 2004. (Section 2.3)

[29] Rogister Y, Valette B : Influence of outer core dynamics on Chandler wobble. in *Forcing of Polar Motion in the Chandler Frequency Band : A Contribution to Understanding Interannual Climate Variations*, éds H.-P. Plag et al., Cah du Cent Eur de Géodyn et de Séismol 24 : 61–68, Walferdange, Luxembourg, 2005. (Section 3.2.2)

[30] Rogister Y, Valette B, Delatre M : Splitting of normal modes by magnetic field. XXIV Assembly of IUGG, Perugia, Italy, 2007.

[31] Rogister Y, Valette B : Influence of liquid core dynamics on rotational modes. Geophys J Int 76 : 368–388, 2009. (Section 3.2.3)

[32] Sasao T, Okubo S, Saito M : A simple theory on the dynamical effects of a stratified fluid core upon nutational motion of the Earth. *In* : Fedorov E.P., Smith M.L., Bender P.L., (eds.), *Nutation and the Earth's rotation.* Dordrecht, Netherlands : Reidel, 165–183, 1980.

[33] Schastok J : A new nutation series for a more realistic model Earth. Geophys J Int 130 : 137–150, 1997.

[34] Scott TC, Aubert-Frécon M, Grotendorst J : New approach for the electronic energies of the hydrogen molecular ion. Chem Phys 324 : 323–338, 2006.

[35] Seidelmann PK : 1980 IAU theory of nutation : the final report of the IAU working group on nutation. Cel Mech 27 : 79–106, 1982.

[36] Smith ML : The scalar equations of infinitesimal elastic-gravitational motion for a rotating, slightly elliptical Earth. Geophys J R astr Soc 37 : 491–526, 1974.

[37] Smith ML : Translational inner core oscillations of a rotating, slightly elliptical Earth. J Geophys Res 81, 17 : 3055–3065, 1976.

[38] Smith ML : Wobble and nutation of the Earth. Geophys J R astr Soc 50 : 103–140, 1977.

[39] Stefani F, Gerbeth G : Asymmetric polarity reversals, bimodal field distribution, and coherence resonance in a spherically symmetric mean-field dynamo model. Phys Rev Lett 94 :184506, doi : 10.1103/PhysRevLett, 2005.

[40] Tanimoto T : Splitting of normal modes and travel time anomalies due to the magnetic field of the Earth. J Geophys Res 94 : 3030–3036, 1989.

[41] Truesdell C, Toupin RA : The classical field theories in "Encyclopedia of Physics", ed. S. Flügge, Vol. 3/1, 226–793. Berlin : Springer-Verlag, 1960.

[42] Valette B : Spectre des vibrations propres d'un corps élastique, auto-gravitant, en rotation uniforme et contenant une partie fluide. C R Acad Sci Paris 309 : 419–422, 1989a.

[43] Valette B : Etude d'une classe de problèmes spectraux. C R Acad Sci Paris 309 : 785–788, 1989b.

[44] von Neumann J, Wigner E : Über ds Verhalten von Eigenwerte bei Adiabatische Prozessen. Phys Z 30 : 467, 1929.

[45] Wahr JM : Body tides on an elliptical, rotating, elastic and oceanless earth. Geophys J R astr Soc 64 : 677–703, 1981a.

[46] Wahr JM : The forced nutations of an elliptical, rotating, elastic and oceanless Earth. Geophys J R astr Soc 64 : 705–727, 1981b.

[47] Widmer R, Masters G, Gilbert F : Observably split multiplets – data analysis and interpretation in terms of large-scale aspherical structure. Geophys J Int 111 : 559–576, 1992

Résumé

Le spectre des modes normaux de modèles de Terre en rotation comprend les modes sismiques, les modes de rotation et le spectre du noyau fluide. Afin de les modéliser, il faut résoudre les équations locales des petites déformations gravito-élastiques de modèles terrestres en équilibre hydrostatique en rotation. Ceux-ci sont obtenus par perturbation de modèles moyens sphériques. Une théorie des petites déformations basée sur la perturbation lagrangienne d'un modèle sphérique est complètement développée. Le travail contient aussi une mise en parallèle des équations locales des petites déformations avec l'approche globale de conservation du moment cinétique de la Terre qui permet d'étudier les variations de la rotation. Une étude numérique des modes sismiques, dont les fréquences sont éclatées par la rotation, et des modes de rotation, en particulier de l'interaction des modes de rotation avec le spectre du noyau fluide, fait apparaître le phénomène de croisement évité des fréquences propres lorsque la structure du noyau fluide est modifiée. Un mécanisme physique plausible est ainsi fourni pour expliquer l'observation d'une fréquence double pour le mouvement de Chandler. L'analogie avec les oscillations d'autres systèmes physiques permet de mieux comprendre l'évitement croisé des fréquences propres.

Mots-clés : Géophysique, géodésie, sismologie, modes normaux, rotation de la Terre, dynamique du noyau fluide

Abstract

The normal-mode spectrum of rotating Earth models is made up of the seismic modes, the rotational modes and the spectrum of the liquid core. The local equations for the infinitesimal elastic-gravitational deformation, based on a Lagrangian perturbation of a spherically-averaged Earth model using the theory of hydrostatic equilibrium, are first established. A comparison is made between this approach and the classical global angular momentum approach to Earth rotation variations. The splitting of the seismic modes by rotation and ellipticity is then computed. Numerical investigation also shows that, by changing the structure of the liquid core, the rotational modes and core spectrum interact to give rise to avoid crossings, which provide a physically plausible mechanism to explain the observed double frequency of the Chandler wobble. The analogy with other oscillatory physical systems allows for a better understanding of the avoided crossing phenomenon.

Keywords : Geophysics, geodesy, seismology, normal modes, Earth rotation, fluid core dynamics